Visualization and Animation of Herman Rings of Rational Functions of Degree 3

by Alan Norton

Introduction

This article is intended to promote understanding and appreciation of some fractal patterns known as Herman rings. Readers are not expected to know a lot of math, but should be familiar with the notion of a complex number and the derivative of a rational function. If you are interested in creating images and animations of Herman rings using these techniques, you will need to be able to program a computer, preferably with a graphics card, and to produce computer images.

This article is not scholarly, it does not contain references or mathematical proofs. If you would like more information or explanation of the concepts in this article, a good place to find that information is in Wikipedia (search in wikipedia.org). Send me a message to my YouTube channel youtube.com/@valannorton if you have any questions or comments.

A Herman ring is a dynamical pattern whereby points in a ring or annulus in the complex plane rotate endlessly through an irrational angle when a rational function (i.e. a ratio of polynomials) is repeatedly applied to them. Herman rings were discovered by the mathematician Michael Herman, who described them in a paper in 1979. Herman rings only occur with rational functions of degree at least 3, and do not occur with polynomials.

Overview

This article describes methods for identifying and visualizing Herman rings obtained from third degree rational functions. These methods involve the following:

1. Defining and constructing Mandelbrot sets for spaces of third-degree rational functions
2. Locating Herman rings when they can be found in these Mandelbrot sets.
3. Identifying spaces of third-degree rational functions where Herman rings are found.

This article considers various families of rational functions of degree three, in which many Herman rings can be found. These families include:

$f_1(z) = z^2(az+b)/(cz+d)$ where $a,b,c,$ and d are complex numbers.

$f_2(z) = m+ z^2(az+b)/(cz+d)$, where a,b,c,d and m are complex numbers.

$f_3(z) = mz(1-z)(az+b)/(cz+d)$, where a,b,c,d and m are complex numbers.

These three families do not include all third-degree rational functions, but they do include all third-degree rational functions of the form $p(z)/q(z)$ where the degree of p is three and the degree of q is one. (These are all the third-degree rational functions that have a superattractive fixed point at infinity; i.e. they map infinity to infinity and their derivative at infinity is zero). All other third-degree rational functions with this property are equivalent to $f_2(z)$ after a linear change of variables.

In addition we consider third-degree rational functions of the form $p(z)/q(z)$ where p is of degree 3 and q is of degree 2. Such functions have infinity as a fixed point ($g(\infty)= \infty$). They are equivalent (after a linear change of variables) to:

$g_1(z)=z(z+a)(z+c)/(bz+1)(z+d)$, and also to

$g_2(z)=z(z+a)(z+c)/(bz+1)(dz+1)$

The functions $g(z)$ (either form) will also be shown to admit Herman rings, which may appear different from the rings associated with $f_1(z)$,$f_2(z)$, and $f_3(z)$.

There are, of course, other degree 3 rational functions p(z)/q(z), where the degree of q is greater than or equal to the degree of p. But these do not really give us anything new, because any such function can be converted to a form of f(z) or g(z) by changing variables by a fractional linear transformation T(z)=(az+b)/(cz+d), i.e. a linear mapping of the Riemann sphere.

In order to make pictures of the Herman rings associated with these families of functions, it is necessary first to determine which values of the parameters a,b,..,m result in a function that has a Herman ring. The methods of finding these parameters that are explained in this article involve generalizing the notion of “Mandelbrot set” to these families of functions, and making images of these generalized Mandelbrot sets.

While finding these Herman rings some interesting patterns become evident, such as:

1. Herman rings can be identified in their Mandelbrot sets by a distinctive pattern of bulbs that appear along curves (hypersurfaces) in their parameter spaces. We call these “MH curves”.

2. Some properties of Herman rings, such as how the ring is distorted from a circular shape, can be identified by properties of the MH curve.
3. Periodic cycles of Herman rings can be found (for any period) by examining the Mandelbrot sets of these functions, in particular for some choices of f(z) and g(z). With a cycle of period P of a Herman ring, iteration of a point in the ring results in a sequence of points that cycle through P distinct rings, while rotating around all P rings, never passing through the same point twice.
4. The interior of these Herman rings can be selected to contain (or not contain) an attractive cycle, depending on the shape of the Mandelbrot set.

Herman rings in families of rational functions can be identified by a pattern that is found in images of their generalized Mandelbrot sets. Animations of evolving Herman rings can be constructed by approximating a curve that follows along that pattern in the generalized Mandelbrot set.

We explore the above families of functions showing many subsets of those families where Herman rings are found. This is not exhaustive: there are many other useful spaces of third-degree rational functions having Herman rings.

1. Technical preliminaries

A. Julia Sets

Julia Sets were discovered in the early 20th century by the French mathematician Gaston Julia [see Wikipedia article], who realized their existence and described them without ever actually seeing them, because he could not calculate them with computers. A Julia set is associated with a formula (rational function), and can be regarded as a picture of that formula.

In this article I will consider Julia sets of rational functions, i.e. formulas that can be expressed as a ratio of two polynomials p(z)/q(z). The degree of such a function is the maximum of the degree of p(z) and q(z). There are many equivalent formal definitions as can be seen in the Wikipedia articles on Julia/Fatou sets. In this article we are concerned with making images that enable visualization of Julia sets. These can often be approximated by the following algorithm:

For each pixel (x,y) in a rectangle in the complex plane, iterate f(z), evaluating the sequence f(z), f(f(z)), f(f(f(z))), … where z is the complex number associated with (x,y). Stop the iteration if the sequence converges to infinity or ends up in a cycle (a finite

number of values that are repeated). Assign a color to the point (x,y) depending on which cycle it converges to, or to infinity, or if the iteration does not get stopped after many iterations. The Julia set is the boundary between the different colored regions.

B. Stable dynamics classification

The mathematician Dennis Sullivan proved that there are exactly four different types of domains (stable domains) that can occur in the complement of the Julia set:

(1) A basin of attraction to a cycle (periodic point). These points converge to the points of the cycle, and the product of the magnitudes of the derivatives of the points in the cycle is less than one. A special case of this is when the derivatives product is zero, referred to as a “super-attractive” cycle.

(2) A basin associated with a parabolic point or cycle. These points converge slowly to a cycle on the boundary of the domain, and the product of the magnitudes of the derivatives of the points in the cycle is exactly one.

(3) A Siegel disc. These points eventually end up in a simply-connected region, where they rotate forever (with irrational angle).

(4) A Herman ring. These points eventually end up rotating forever (through an irrational angle) in a shape topologically equivalent to an annulus, each point rotating about a closed curve.

Examples of the first three of these can easily be found when f(z) is the quadratic polynomial $z^2 + M$. Herman rings however require that f(z) be a rational function (not a polynomial) and to be of degree at least 3. The goal of this article is to describe a number of techniques for calculating images and animations of Herman rings with degree 3 functions.

C. Winding numbers, Siegel discs, and Herman rings.

The dynamics of the polynomial $p(z) = e^{2\pi i \theta}z(1-z)$ depends strongly on the value of θ. If θ is irrational, and if θ is not easily approximable by rational numbers (in a sense that it is the limit of a sequence of rational numbers whose denominators do not grow too fast) then there is a Siegel disc at the origin in the complex plane, such that the result of applying p(z) on points in that disc is equivalent to a rotation by the angle θ. Otherwise,

i.e. for other angles θ, there is a parabolic domain associated with f(z). Herman Rings are similar, in that the action of p(z) is also equivalent to an irrational rotation, however this rotation is of an annulus, not a disc. There is similar behavior with both Herman rings and Siegel discs: These occur only with irrational rotations that are not easily approximated by rational numbers. That rotational angle is called the winding number. Most irrational winding numbers do in fact occur with Siegel discs and Herman rings, in the sense that the complement of such winding numbers has measure zero.

D. Mandelbrot sets.

The classic Mandelbrot set (named after Benoit Mandelbrot) is calculated by iterating the quadratic polynomial z^2+m, with starting value z=0, with values of m obtained from the complex coordinates of points in a region of the complex plane. The Mandelbrot set is the set of points m for which the iteration remains finite. An alternate (lambda) version of this set uses the function $\lambda(z)= mz(1-z)$ with starting value z=0.5. The significance of the values z=0 and z=0.5 is that these are the critical points of the functions; i.e., points where the derivative vanishes.

A theorem of Dennis Sullivan states that each stable domain of a rational function contains at least one critical point. Consequently the Mandelbrot set identifies the stable domains of quadratic polynomials, thereby providing a picture of the dynamics of the various quadratic polynomials. We can regard the Julia set as a picture of its defining formula, and the Mandelbrot set as a picture of the set of all quadratic formulas.

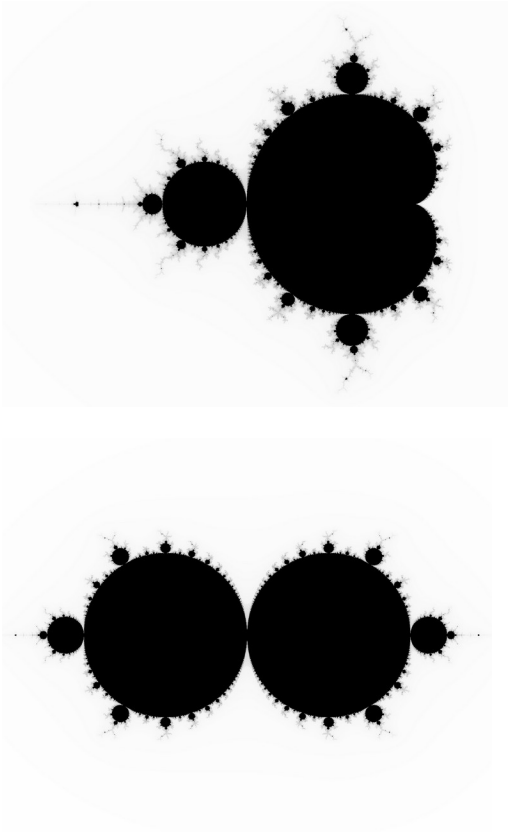

Fig 1: Classic Mandelbrot set for z^2+m (first), and the Mandelbrot set in lambda coordinates for $mz(1-z)$ (next). Points colored black correspond to polynomials whose critical point remains bounded under iteration. White points correspond to polynomials whose critical point diverges to infinity when iterated. The different black bulbs correspond to cycles with different periods. The central heart-shape of the Mandelbrot set is called the "cardioid".

E. Generalization of the Mandelbrot set

For the understanding of Herman rings, or for the classification of dynamics of spaces of rational functions, it is useful to generalize the Mandelbrot set to make pictures of spaces of rational functions. The classic Mandelbrot set classifies polynomials by classifying the result of iterating their critical points. Given Sullivan's theorem (above) a similar classification will be useful for other spaces of rational functions. However, it is bound to be more complicated, because each rational function can have several critical points, and because the results of iterating these

critical points can be more complicated than identifying whether or not the iteration converges to infinity. Another complication is the fact that we are often dealing with spaces of functions having two or more complex dimensions.

The classic Mandelbrot set can be regarded as a means of classifying quadratic polynomials, labeling them according to their limiting behavior as one iterates the critical point. Each bulb of the Mandelbrot set identifies polynomials having a particular period in an attractive cycle. Points on the boundary of the Mandelbrot set correspond to polynomials with a parabolic point, or polynomials which iterate forever into a Siegel disc, without having an attractive cycle.

Similarly we can divide a space of rational functions into subsets based on the results of iterating the critical points of the functions. The result of the iteration is that either one or more critical points iterate forever without landing in an attractive cycle (i.e. they land in Siegel discs or Herman rings) or all critical points are attracted to periodic cycles, possibly including attraction to infinity. If we use different colors to identify the various patterns of cyclic behavior that occur with the critical points, then we partition the space of functions into a set of bulbs with different cyclic patterns, with points on the boundaries of these bulbs corresponding to Siegel discs and Herman rings. Of course, we cannot easily draw these sets when there is more than one complex dimension to the space, but we can intersect the space with complex planes, identifying bulbs in each plane.

For our purposes we shall call a “Generalized Mandelbrot set” any partitioning of a space of rational functions based on classifying the critical points of the functions according to their cyclic behavior or limiting behavior (if they do not all converge to an attractive cycle). These Mandelbrot sets can be visualized in planar sections, and often we can animate the planar sections to show higher dimensional patterns. These generalized Mandelbrot sets are shown and animated later in this article.

The above classification requires an algorithm to determine when a sequence of iterates converges to a periodic cycle. A simple way to do this is as follows: Suppose that we are iterating each critical point N times (typically N is 100000 or more). At N/2 iterations we save the value of the iterated critical point. Then, for each subsequent iteration, the saved point is compared

with the new iteration. If the difference is very small, there is a cycle of length the difference between N/2 and the subsequent iteration count.

For an example of this use of a generalized Mandelbrot set, consider the set of functions $f(z)= x^2(ax+b)/(4x+d)$ where a, b and d are complex numbers. For each angle θ let $a=d=e^{i\theta}$. For each value of θ there is a complex plane of values $(a,b,d)= (e^{i\theta},b, e^{i\theta})$ through the complex 3-space of functions f(z). The following image shows the Mandelbrot set in that plane, with theta about 110 degrees:

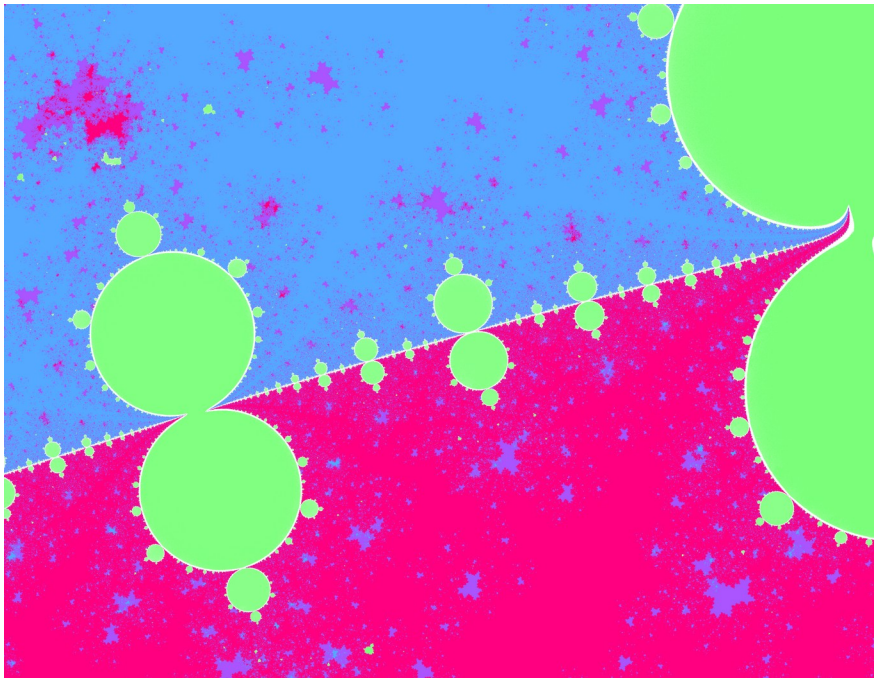

Fig. 2: A generalized Mandelbrot set for the functions $f(z)= x^2(ax+b)/(4x+d)$, intersected with a planar slice of $a=d=e^{i\theta}$, with a constant θ of about 2 radians. A portion of the planar slice is illustrated.

In the above image (here the center of the image is $b=4e^{i\theta}$), points are colored red if both critical points converge to zero, blue if they both converge to infinity, violet if one goes to infinity and one to zero, green if both critical points converges to a cycle, and white if a critical point does not go to any cycle. This can be animated by moving θ from π to π/2, moving the b-plane with theta, resulting in the video "A trip around a Mandelbrot set for Herman Rings". Later we shall show how that path in the Mandelbrot set was calculated.

F. Spaces of 3rd degree rational functions

A third-degree rational function can be expressed as a ratio of polynomials p(z)/q(z) where p and q are of degree no greater than 3 (and at least one of them is of degree 3). In this article we are first going to consider the case where p is of degree 3 and q is of degree 1 or 2. Any of these rational functions is equivalent to the functions

$z^2(z+b)/(cz+1) + m$ or

$z(z+a)(z+b)/(cz+1)(dz+1)$

by a linear change of variable. Therefore these spaces of functions have complex dimensions 3 and 4.

G. Computation

In recent years, graphics cards have become cheap and widely used because of their use in playing computer games. The graphics processor (GPU) can include thousands of processing nodes. These GPU's are readily applied to calculating Julia sets and Mandelbrot sets because that calculation often involves millions of repeated floating point operations that can be applied independently and identically to determine the different pixels in an image. All of the images and animations of this article were calculated on a laptop with a recent NVidia GPU. The Nvidia CUDA software was programmed to repeatedly iterate specified rational functions applied to the points of the images.

H. Computational accuracy vs. mathematics

One may question the value of using computers to calculate dynamics. For example, mathematics tells us that Herman rings and Siegel discs have the property that the rotation angle must be an irrational value and, in fact, a value not easily approximated by rationals. Floating point values in a computer (of any precision) are never irrational. If a mathematical point in a Siegel disc or Herman ring is iterated it will never return to its original starting value. However, in a computer approximation of a Siegel disc or Herman ring, any point when iterated will eventually end up in a cycle, because there are only a finite number of values in the computer representation of complex numbers.

This criticism is however not as serious as it appears. These calculations are always approximations, and the better the

approximation, the better the result. When coefficients of a rational function are very near the values associated with a Herman ring, then iterates of the resulting function will approximate that Herman ring, in the sense that iteration of points in the ring will stay in the ring for very many iterations. If a critical point of a formula can be iterated millions of times without diverging from a ring, then we can expect calculations of the associated Julia set to be accurate when fewer than a million iterations are used in its calculation. One must always be vigilant about the accuracy of these calculations, especially when unexpected artifacts show up in the resulting images. You can create images of Julia sets and Mandelbrot sets that are indistinguishable to the naked eye from the true shapes by appropriately adjusting the number of iterations and the accuracy tolerances.

2. Herman Rings from $x^2(x+a)/(1+\underline{a}x)$

The easiest way to find Herman rings is to use the formulas $f_a(x) = x^2(x+a)/(1+\underline{a}x)$, with complex values of a. The underscore is used to indicate complex conjugation. The linear fractional transformation (LFT) in this formula, $(x+a)/(1+\underline{a}x)$, has the property that it maps the unit circle to itself. It is also symmetric under the inversion $i(x) = 1/\underline{x}$ which reflects points in that circle. In the formula $f_a(x)$, the multiplication of the LFT by x^2 has the effect of making both zero and infinity super-attractive, while preserving the invariance of the unit circle.

We can better understand the dynamics of $f_a(x)$ by calculating the Mandelbrot set of this set of mappings as follows:

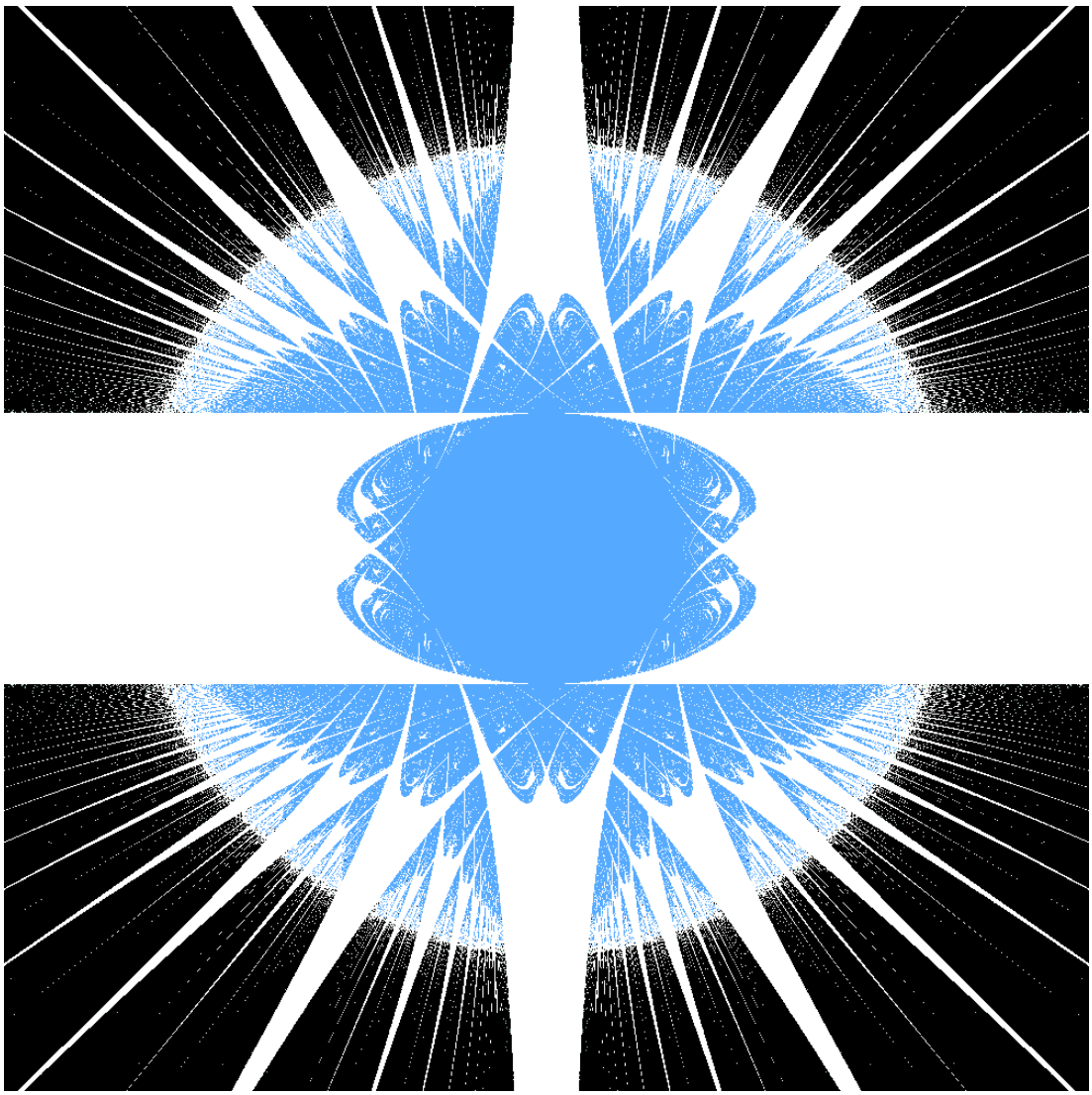

Fig.3: A Mandelbrot set of $x^2(x+a)/(1+\underline{a}x)$ illustrating the *a*-plane centered at the origin.

In the above image, points are colored blue if the iteration of the two critical points converges either to zero or infinity. White indicates the critical points converge to a finite cycle. The remaining (black) points iterate 10000 times without getting into a cycle, which indicate the likely existence of a Herman ring. This image is centered at the origin, of size 8x8. Note that all the Herman rings occur outside the circle of radius 3. The white shapes that narrow as they extend outward correspond to values of *a* that are associated with rational rotation numbers about the unit circle.

Note that the above image does not bear much resemblance to the classic Mandelbrot set. That is because the formula $f_a(x)$ is not a complex analytic function of *a*, due to the fact that it depends on both

a and $\underline{a}$. We shall see later generalized Mandelbrot sets of complex analytic spaces of functions that more strongly resemble the shapes in the classic Mandelbrot set.

To calculate a Julia set having a Herman ring, one can select a to be one of the points colored black in the above Mandelbrot set, and iterate the associated $f_a(x)$, as in the following:

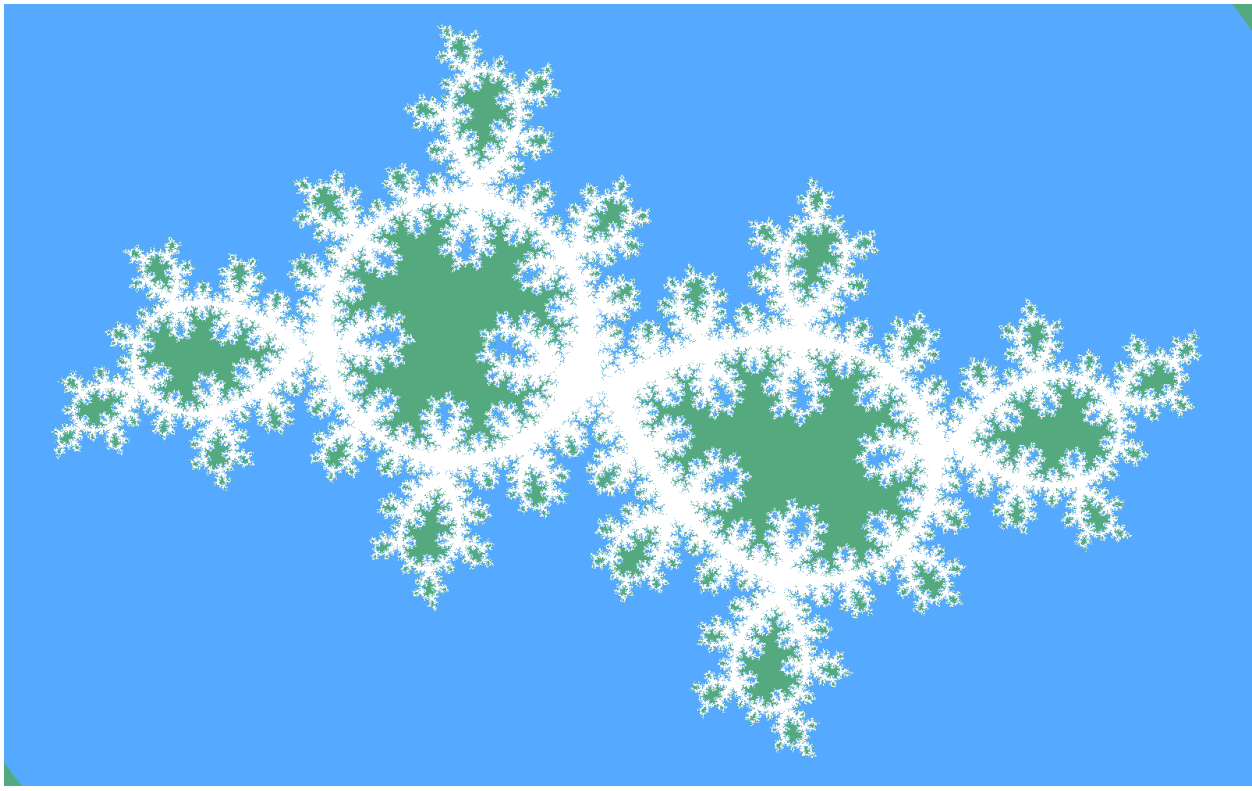

Fig. 4: A Julia set of $x^2(x+a)/(1+\underline{a}x)$

In the above image, a value of a has been chosen so that $|a|=3.1$ and such that the rotation number of $f_a(x)$ about the unit circle is approximately the golden ratio,

$(\sqrt{5}-1)/2$. The points colored blue converge to infinity, those colored green converge to zero, and the white points eventually end up in a circular Herman ring centered at the origin.

People often use the golden ratio as a winding number because it is known to be associated with Herman rings and Siegel discs. In some sense it is the irrational number most difficult to approximate with rationals. However the winding numbers that result in Herman rings are in fact quite common, they form a set whose complement has measure 0. Note also the preponderance of black (corresponding to Herman rings) in the Mandelbrot set of figure 3 when $|a|$ is large.

To see how the Julia sets of $f_a(x)$ vary as the value of a varies, see the animation "A tour of Herman rings". In that animation the parameter *a* is moved about the origin along the circle of radius 4 with its angle varying from 0 to $\pi/2$. At rational winding numbers the inside and outside shapes touch at a number of points equal to the denominator of the winding number. In between these values, points converging to a Herman ring are colored black.

3. Herman rings from the formula $g_a(x) = z^2(z+a)/(1-\underline{a}z)$

Although $g_a(z)$ differs by only a minus sign from the formula for $f_a(z)$, it produces very different Herman rings. The following is its Mandelbrot set, rotated by 90 degrees:

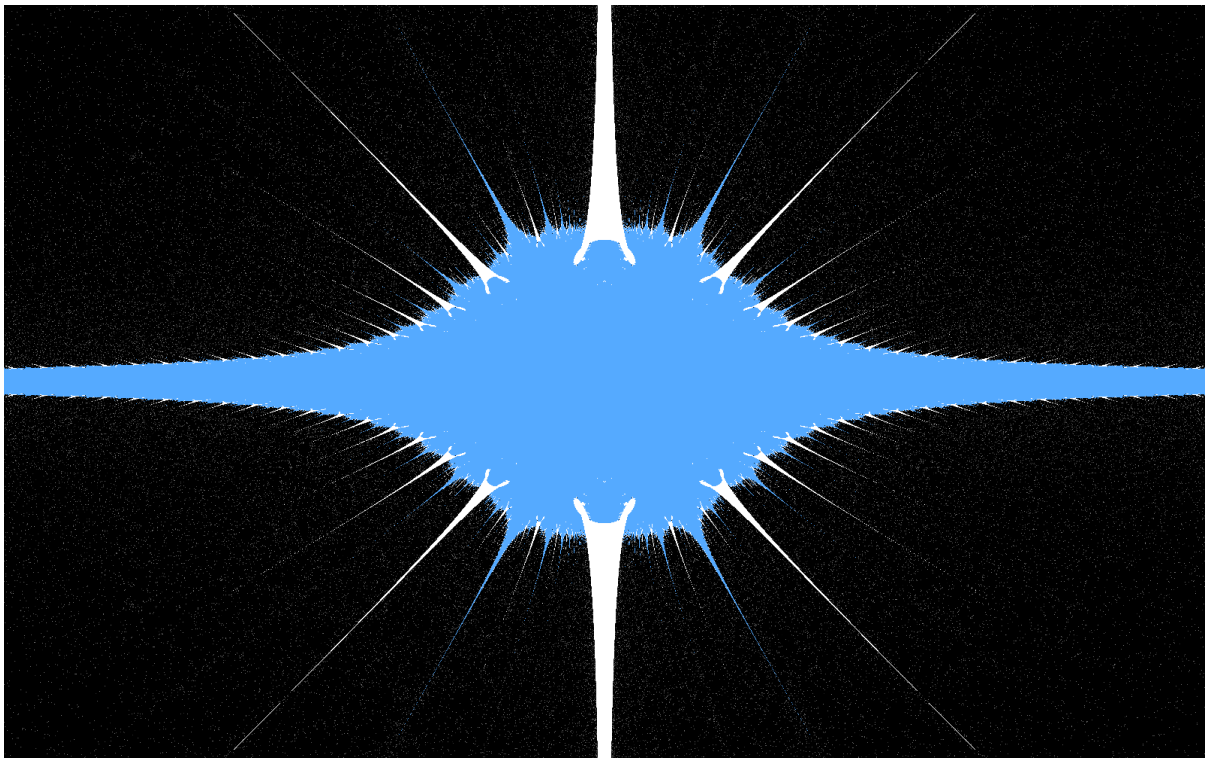

Fig.5: Mandelbrot set of $z^2(z+a)/(1-\underline{a}z)$ illustrating the *a*-plane centered at the origin.

Again, the values of *a* associated with Herman rings are colored black, blue points converge to zero or infinity, and white points converge to cycles. An example Julia set of $g_a(z)$ with a Herman ring is shown below:

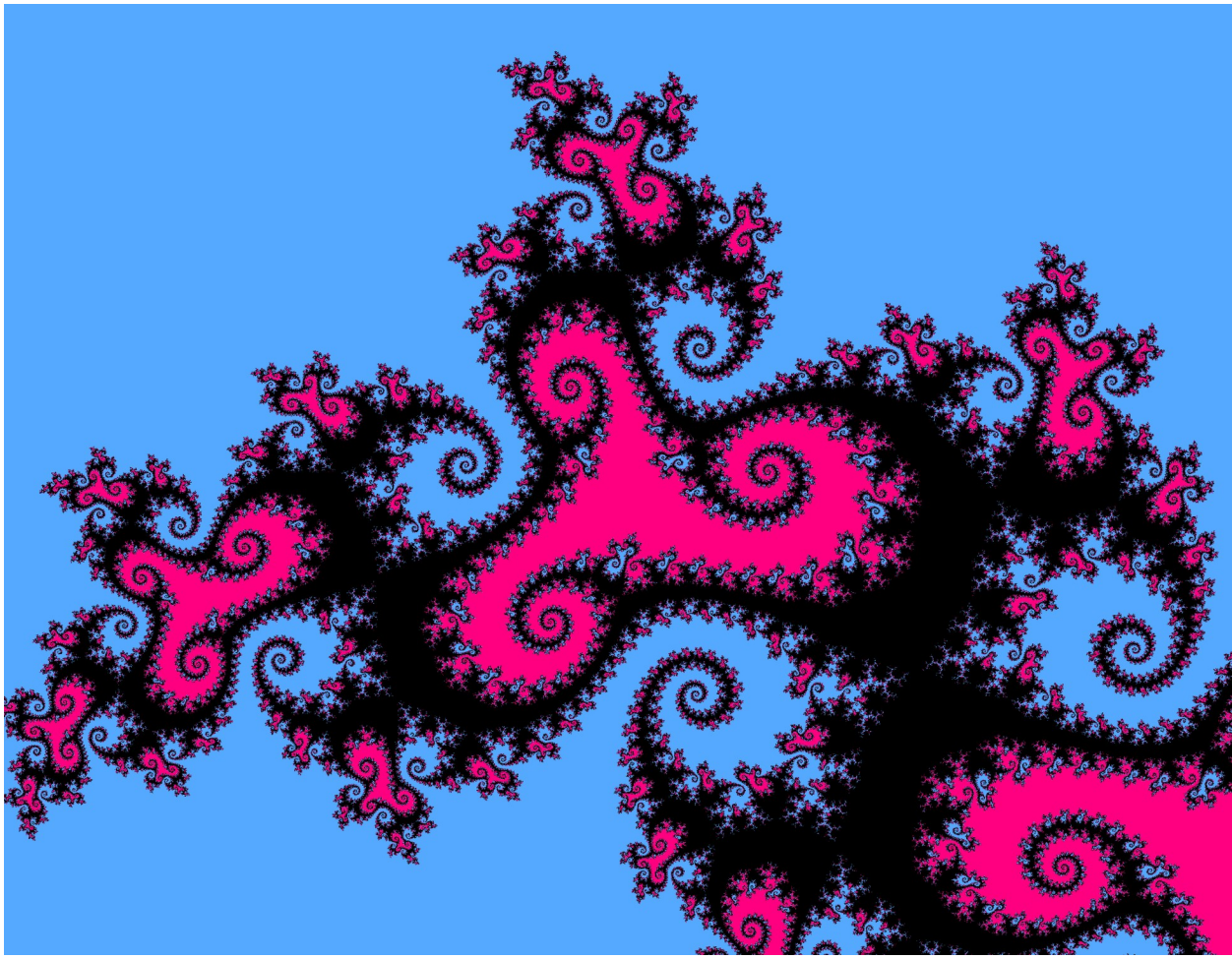

Fig 6: A Julia set of $z^2(z+a)/(1-\underline{a}z)$. Points colored black eventually end up in a Herman ring that encloses the red triple spiral at the center.

The Herman rings and Julia sets resulting from $g_a(z)$ can be animated, by animating the parameter *a* following a path in the black region of figure 5. For an example of this, see the video "Wiggly Rings".

4. Principal Observations

In the discussions that follow we shall be showing some techniques for using complex analytic Mandelbrot sets to identify Herman rings and properties associated. In the process of finding these techniques I have identified methods and visual features that helped me understand how to calculate these sets. I am calling these "Observations" because, while they are not mathematically proven, they can be reliably used in computing Julia and Mandelbrot sets.

1. Functions having Herman rings are found to occur in their Mandelbrot set along smooth (real) hypersurfaces, in a pattern

where cyclic bulbs are arranged on both sides of the surface, positioned according to the winding numbers of the Herman rings. I shall refer to this surface (or the curve of its intersection with a complex plane) as a Mandelbrot-Herman surface or curve, or for short, the *MH curve* or *MH hypersurface*. In every case described here, there is an MH hypersurface, of real codimension 1 in a larger complex space of rational functions. They are called MH curves because we always visualize them as curves in complex planar slices of the larger complex space.

An MH curve is shown below alongside an image of the classic Mandelbrot set.

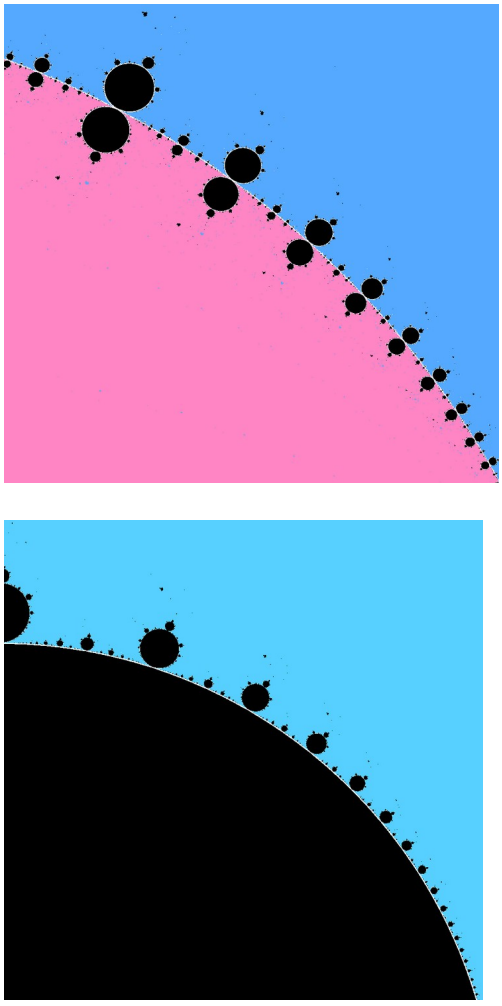

Fig 7: An image of an MH curve (first) next to an image of a portion of the classic Mandelbrot set (next). In the first image, points that converge to a point in the center of the Herman ring are colored red. In both images, points converging to infinity are colored blue, points converging

to other cycles are black, and points that do not converge to cycles are colored white.

Note the similarity of this MH curve to the edge of the classical Mandelbrot set, where Siegel discs are located. Both shapes have a similar pattern of attached bulbs, but the MH curve has bulbs on both sides of the curve. In every generalized Mandelbrot set that I have seen, the MH pattern is associated with functions having Herman rings.

2. It appears that whenever a function has a Herman ring, at least two of its critical points eventually iterate into the ring. This helps distinguish MH curves in Mandelbrot sets from other curves, such as the edges of bulbs identifying functions with Siegel discs.
3. There are three (real) parameters, or parameterizations of points, in all the MH surfaces I have found. These include: (1) The winding number, which increases or decreases along the curve, and has rational values at the points where the bulbs are attached. (2) The thickness of the Herman ring, and (3) an angular parameter I call "alignment". Adjusting the alignment causes the shapes in the interior of the Herman ring to rotate (around the ring center) relative to the shapes on the exterior of the Herman ring. The alignment parameter can be seen in the appearance of the MH curve near points of rational winding number. When the inner and outer shapes are aligned, the bulbs on opposite sides of the MH curve meet at a point along the curve. When the shapes are not in alignment, the bulbs on opposite sides separate from the curve.

5. Mandelbrot sets of $z^2(az+b)/(cz+d)$

The previous two example formulas are special cases of the rational functions $z^2(az+b)/(cz+d)$, with complex coefficients a,b,c and d. This formula can be simplified to $f_{bc}(z) = z^2(z+b)/(cz+1)$ by changing variables, multiplying z by a complex constant p, with $p^2 = d/a$, then dividing numerator and denominator by d. The change of variables converts the original formula to $z^2(z+b)/(cz+1)$. This is a complex two-dimensional space of functions. We can explore the Mandelbrot set of this space with the purpose of identifying the values of b and c that result in Herman rings. Note that the roles of b and c are symmetric: Swapping b and c has the effect of inverting $f_{bc}(z)$ in the unit circle, replacing z with 1/z.

To get an overview of this Mandelbrot set, we can calculate planar sections for different values of c . Illustrated are the b-planes when c= 2, 3, 4, and 20. Note that there is an MH curve for c = 3, and as c increases this becomes more sharply defined. When c = 20, the green-colored portion of this Mandelbrot set strongly resembles the lambda form of the classical Mandelbrot set in Figure 1, except that the interior of the left circle has interior bulbs that are reflections of the outside bulbs.

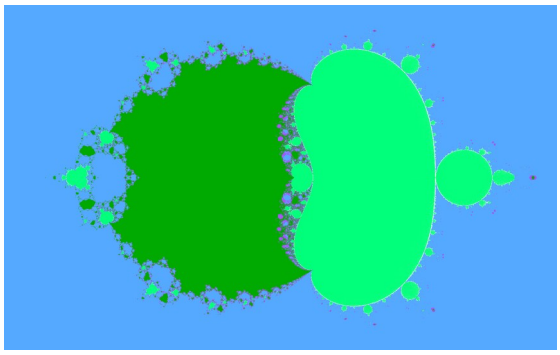

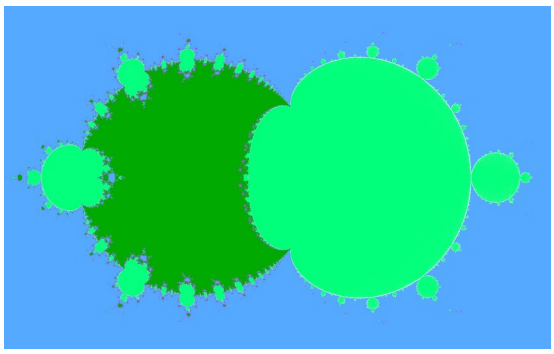

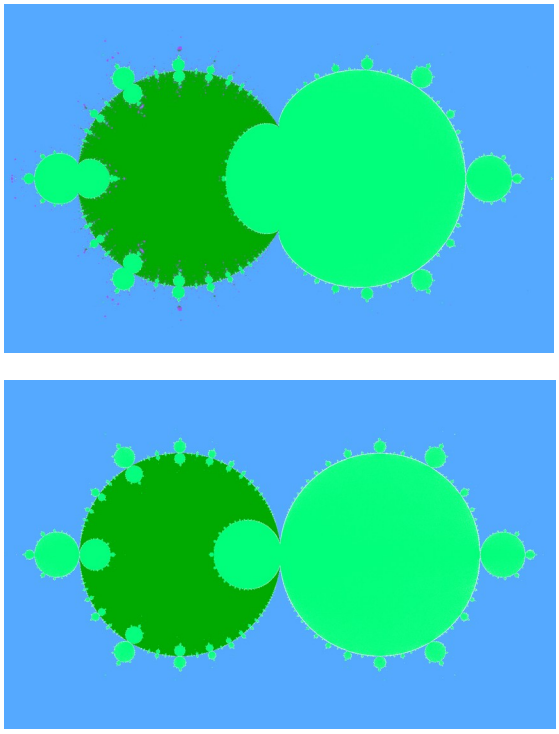

Fig 8: Four different slices of the Mandelbrot set of $f_{bc}(z) = z^2(z+b)/(cz+1)$, with c = 2, 3, 4, and 20. Points are colored blue if both critical points go to infinity, dark green if both go to zero, lighter green if the critical points are attracted to cycles, and purple if critical points go to both zero and infinity. Otherwise the point is colored white.

Overall we can see that an MH curve can be found whenever $|c| > 3$, and it becomes circular as $|c|$ becomes large. When points are selected from the MH curve, the corresponding Julia sets exhibit Herman rings that increase in thickness as $|c|$ increases above 3, decreasing to zero width as $|c|$ approaches 3.

The alignment parameter can be illustrated by moving c around a circle, for example choosing $c = 5e^{i\theta}$ as θ varies from 0 to 2π. We find that, as θ varies, the various opposing bulb-pairs along the MH ring twist and separate into two shapes similar to the classic Mandelbrot set, and then these two merge back into opposite bulb pairs.

The following sequence illustrates this separation occurring at a 3-cycle bulb:

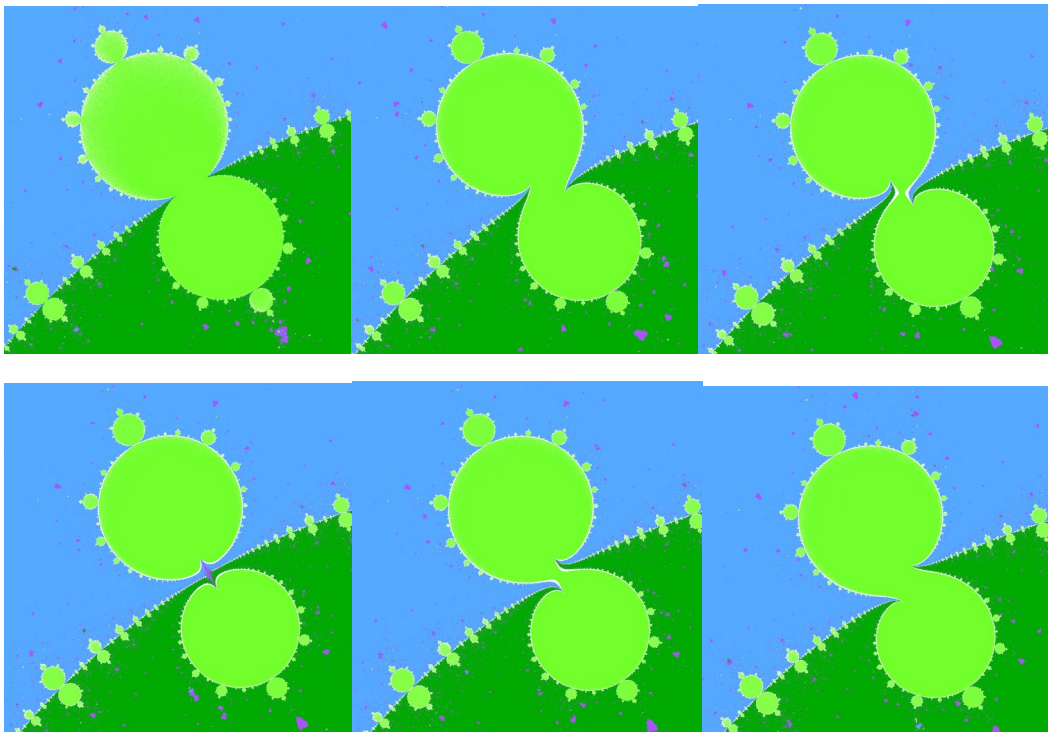

Fig 9: 6 stages in the separation and rejoining of the bulbs associated with the rational winding number of ⅓ , using $z^2(z+b)/(cz+1)$, with $c = 5e^{i\theta}$, with 6 values of θ between 0 and $\pi/3$.

The separation and rejoining of the bulbs has an obvious effect on the Julia sets of $f_{bc}(z)$ when $c = 5e^{i\theta}$, as θ varies. This modifies the alignment of shapes inside and outside the Herman ring. As θ increases, the interior of the Herman ring rotates clockwise relative to the exterior, as seen below:

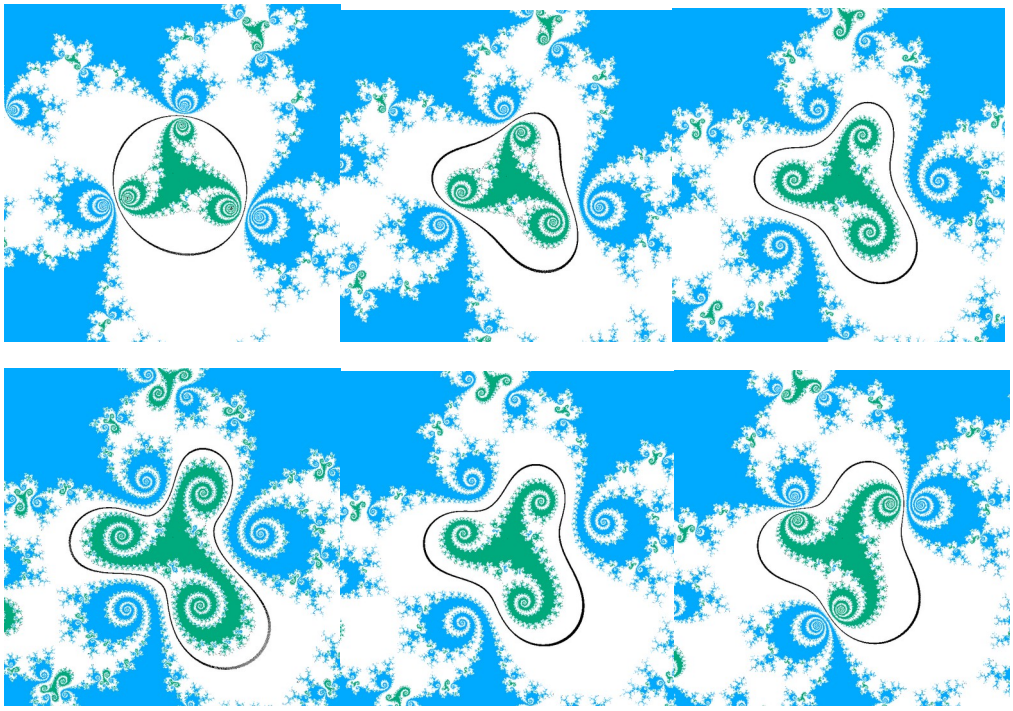

Fig. 10: Julia sets with Herman rings of winding number slightly larger than ⅓, with $c = 5e^{i\theta}$, for the same values of θ as were used in figure 9. The curves in these images show paths followed by points in the Herman ring.

At the point in the MH curve where the inner and outer bulbs separate, i.e. when the alignment is completely backwards, the Herman ring in the Julia set disappears. This results in merging of the inner and outer spirals, resulting in the following Julia set:

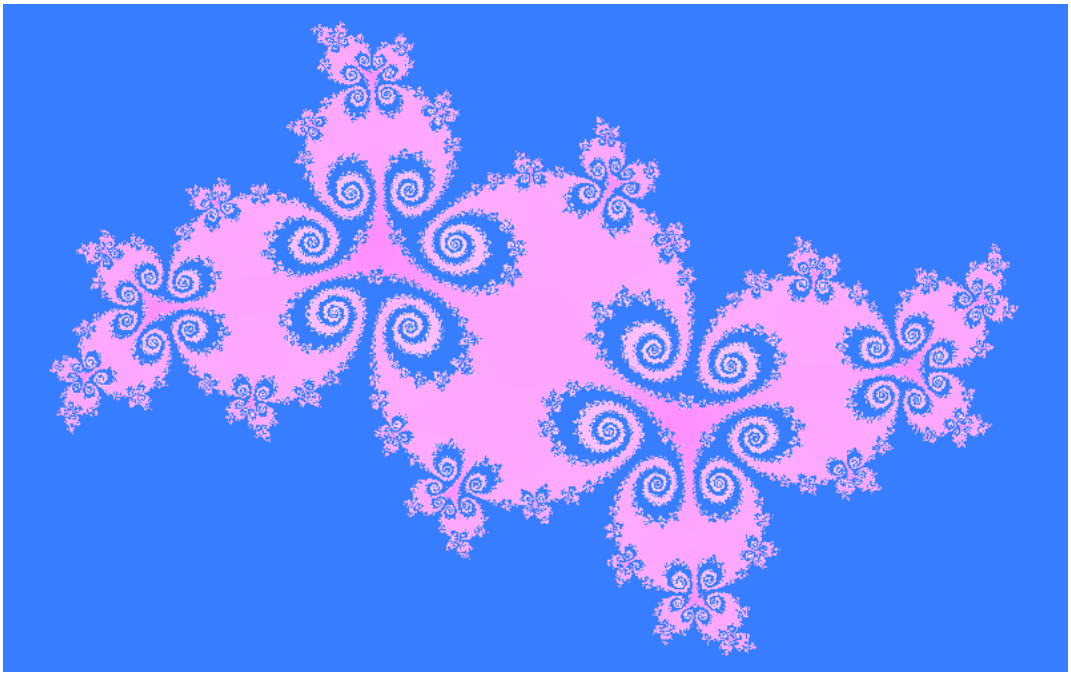

Fig. 11: A Julia set where the winding number is ⅓, and with θ chosen so that the inner and outer bulbs of the MH curve have separated, selected from the center of the fourth image of figure 9.

More generally, for each rational winding number p/q, the associated bulbs of the MH curve separate q times as θ goes from 0 to π. In the corresponding Julia sets, these separations coincide with degeneration of the Herman rings when the inner and outer spirals collapse. Even though the separations are frequent when q is large, the interval of θ values where the MH curve separation occurs is so narrow so that the separations are not easy to find in images of MH curves, unless they are greatly magnified.

The Mandelbrot sets of figures 3 and 5, $z^2(z+a)/(1+\underline{a}z)$ and $z^2(z+a)/(1-\underline{a}z)$, can be visualized embedded in the generalized Mandelbrot set of $f_{bc}(z) = z^2(z+b)/(cz+1)$. However, to visualize this in complex planar images, the planar slice of complex 2-space changes as the value of a is changed. For each complex number a we can calculate the Mandelbrot set's intersection in the complex plane of points $b = a+p$ and $c = \underline{a}+p$, for a rectangle of complex values of p near the origin. For the formula $z^2(z+a)/(1+\underline{a}z)$, this is illustrated in the video "Into the Herman Ring cusp M-Set", where a follows the circle of radius 3, starting at a value with winding number $(\sqrt{5}-1)/2$, the golden ratio, and continuing to a nearby cusp.

For the formula $z^2(z+a)/(1-\underline{a}z)$, this is illustrated in the video "A Trip around a Mandelbrot set for Herman Rings", where the complex number *a* follows the circle of radius 4 from the angle π to 2π . At each rational winding number p/q, the bulb-pairs on the MH curve separate when q is odd. When q is even, there is no separation and the inner and outer shapes of the Julia sets are aligned.

An algorithm for tracking MH curves.

In order to visualize Herman rings and how they change as their formula changes, it is useful to determine a path in the space of formulas that follows an MH curve. It is very easy to follow such a path for the functions $g_a(z)$ and $f_a(z)$, by animating the parameter *a*. However, for other families, like $f_{bc}(z) = z^2(z+b)/(cz+1)$, it can be difficult to find such paths because it is not clear if there is an analytic expression for values of *b* and c that follow the MH curve. In this section I describe an algorithm for calculating such paths

One should note that, to obtain excellent images of Herman rings, it is not necessary to have an exact expression for the values of parameters defining the formulas that result in a Herman ring. It is sufficient to find parameter values such that a large number of iterations of the critical points of the formula do not result in convergence to a cycle or infinity. If, for example, you would like to create images of Herman rings using 100000 iterations in the image calculation, then it suffices to find parameter values such that the critical points do not iterate into a cycle after 100000 iterations. This observation is useful in interpolating curves that follow MH curves.

To approximate an MH curve we start with two points positioned approximately on the curve. Such points can be manually identified by selecting a rectangle that contains a desired portion of the MH curve, such as figure 7 above. Then, repeatedly, decrease the size of the rectangle while increasing the number of iterations used (typically by a factor of 2-5 each time). The image will need to be re-centered on the MH curve as the rectangle size is reduced. When the size of the image (in complex numbers) is less than 10^{-8}, it will be necessary to use double precision in the iteration. Stop this process when the number of iterations is sufficiently large for the desired accuracy. (Typically I stop this process at 1000000 iterations).

Given two points along the MH curve we need an algorithm to find a point on the MH curve that approximately bisects the curve between the two starting points. First we bisect the straight line between the two points and choose a small rectangular grid centered at the

midpoint, aligned with the line between the points. The grid extents should be 1/10 the distance between the two points or less, and of fairly low resolution, say 100x100. Calculate the Mandelbrot set on this grid, distinguishing the points on the grid for which the iteration of at least two critical points do not converge to a cycle. Check the grid for horizontal rows of distinguished points, and select a point in the middle of such horizontal rows. Then repeat this process, reducing the grid extents by a factor of two and doubling the number of iterations. This search is terminated when the number of iterations reaches the maximum desired, say 1000000. Assign a valid bit of 'True' if the search is successful. If this search does not terminate successfully (e.g. a horizontal line of distinguished points is not found), set the valid bit to 'False'.

The search for a bisecting point is repeated recursively, each time dividing the interval between two points and searching for a midpoint on the MH curve. This continues between each pair of adjacent points for which at least one has a 'True' valid bit. The bisection is terminated when adjacent points are sufficiently close, typically it is stopped when the adjacent points are closer than 0.001 of the distance between the original starting points.

At completion of the above algorithm, discard all points with a 'False' valid bit. The approximate MH curve is then obtained by linearly interpolating along the sequence of points that have been found.

It is usually necessary to correct errors resulting from the above algorithm, for three reasons: First, when the bulbs along the MH curve separate as in figure 9, the algorithm may not follow the curve approaching the separation. Second, this algorithm can follow Siegel discs that occur along the outside of bulbs beside the MH curve. Third, when there is a rational rotation number with a small denominator, the MH curve may be interrupted for a short interval, as in the first image of figure 9. When errors like these three are observed, one can discard the points that are in error, and then repeat the search algorithm to fill in between pairs of points as needed.

Note that the above algorithm can be used to follow MH curves through higher dimensional spaces if the starting and ending points are not in the same complex plane. For example one can follow the MH curve for $f_{bc}(z) = z^2(z+b)/(cz+1)$ when the values of b and c both change between the starting and ending points of the MH curve. Regardless of the starting and ending points, there is a complex plane that contains them. Let p and q be the starting and ending points in $\mathbf{C}^2$

, complex 2-space. Then the complex plane containing these two points can be parameterized by $(1-r)p + rq$, for complex numbers r. This plane contains p and q when r assumes the complex numbers 0 and 1. The MH curve can be tracked (using the above algorithm) in that complex plane, resulting in a sequence of points in $\mathbf{C}^2$ that follows along the MH curve. This technique can also be used to track the MH curve through higher dimensional spaces, if for example we are using the Mandelbrot set of a family of functions with more than 2 varying complex coefficients.

For an example of following an MH curve, using the above algorithm, see the Julia set animation "Rolling 3-spirals along a Mandelbrot set for Herman Rings". In this case the Julia sets of $f_{bc}(z) = z^2(z+b)/(cz+1)$ are animated by following b and c parameter values near a point where the MH curve approaches a degeneracy at winding number ⅓.

6. Mandelbrot sets and Herman rings of $m+ z^2(az+b)/(cz+d)$

The formula $f_2(z)=m+ z^2(az+b)/(cz+d)$ provides a space of three complex dimensions in which it is possible to find Herman rings that cannot be found in the space of functions $f_{bc}(z)$ above. In this space are various periodic cycles of Herman rings (of any period whatsoever). We can also find Herman rings for which the interior of the ring does not contain an attractive fixed point. All the Herman rings associated with functions $f_{bc}(z)$ have a connected domain of points attracted to the origin in the interior of the ring.

In order to show the Herman rings in this space we provide a description of the Mandelbrot set for these functions, showing how MH rings can be found. These can be used to construct animations of Julia sets with associated Herman rings. We have found three different parameterizations of these functions to be useful in finding MH curves in their Mandelbrot sets, either

(1)$f_2(z)=m+ z^2(z+b)/(z+d)$ when $|b-d|$ is small, and
(2)$f_2(z)=m+ z^2(z+b)/(cz+1)$ with b and c of magnitude larger than 3.

A Mandelbrot set for $f_{bdm}(z)$

With a linear change of variables we can represent all functions of the form $m+ z^2(az+b)/(cz+d)$ as $f_{bdm}(z) = m+z^2(z+b)/(z+d)$, with complex numbers b, d and m. The formula $f_{bdm}(z)$ approaches the standard quadratic $m+z^2$ as b approaches d. As a result, when b is very near d, the Mandelbrot set of $f_{bdm}(z)$ is very close to the classic Mandelbrot set of quadratic polynomials, when restricted to the complex plane of values (b,d,m) with complex numbers m. For the following discussion

we will distinguish between the “classic Mandelbrot set” which is the Mandelbrot set of quadratic polynomials in the complex plane, and the “generalized Mandelbrot set” which is the Mandelbrot set of $f_{bdm}(z)$ in complex 3-space, whose intersection with the plane of values (b,d,m) approximates the classic Mandelbrot set as |b-d| approaches 0.

It will be useful to replace b and d with a polar representation. We represent b-d in polar coordinates as $2\varepsilon e^{i\varphi}$ where |b-d| = 2ε, and represent b+d as $2re^{i\theta}$ where |b+d| = 2r, where θ and φ are real values between 0 and 2π, and r and ε are real numbers. This way $g_{bdm}(z)$ becomes $m+z^2(z+re^{i\theta}+\varepsilon e^{i\varphi})/(z+re^{i\theta}-\varepsilon e^{i\varphi})$. We shall see that, when ε is small, this representation enables us to see how the shape of the Mandelbrot set of $g_{bdm}(z)$ varies nearby the classic quadratic Mandelbrot set.

Consider the animation “Herman Rings on the Edge of the Mandelbrot Set” . In this video, we are viewing the intersection of the Mandelbrot set of $f_{bdm}(z)$ with the complex plane of values (b,d,m). Initially ε is zero, giving the classic Mandelbrot set. Then ε is gradually increased to 0.0001 with r = 0.5, and with the angles θ and φ equal, increasing from zero to π/2 during the animation. We see that, along the edge of the (classic) Mandelbrot set, there is a pair of bulges that slide along the edge as θ and φ increase. In between the two bulges can be seen an MH curve, indicating that Herman rings can be found here.

In that video, when θ and φ reach π/6, the value of θ is held constant while φ increases a full revolution (2π) , then θ and φ continue to increase together for the duration of the video.

Structural patterns in the Mandelbrot set of $f_{bdm}(z)$

Because this set sits in complex 3-space it is difficult to describe it completely. However, one way to describe it is as a set of planar shapes, varying r, θ, ε, and φ while observing its intersections with the plane of values (b,d,m), initially considering only small values of ε, say ε<0.01. For such small values of ε, this Mandelbrot set’s intersection with the plane is similar to the classic Mandelbrot set. With larger ε, that comparison becomes difficult and it becomes challenging to identify Herman rings in that larger space.

One important shape occurring in this planar space is what I call “mandelbirds”. These are shapes that resemble the classic Mandelbrot set but may be slightly distorted. Mandelbirds do occur in the classic Mandelbrot set, as “islands”, separated from the central shape of the classic Mandelbrot set (although these shapes are in fact connected to

the main body, but only by a curve). There are in fact many mandelbirds near each bulb of the classic Mandelbrot set. The interiors of Julia sets of points from such mandelbirds contain infinitely many separated components. For example, the following mandelbirds are nearby the 3-cycle bulb of the classic Mandelbrot set:

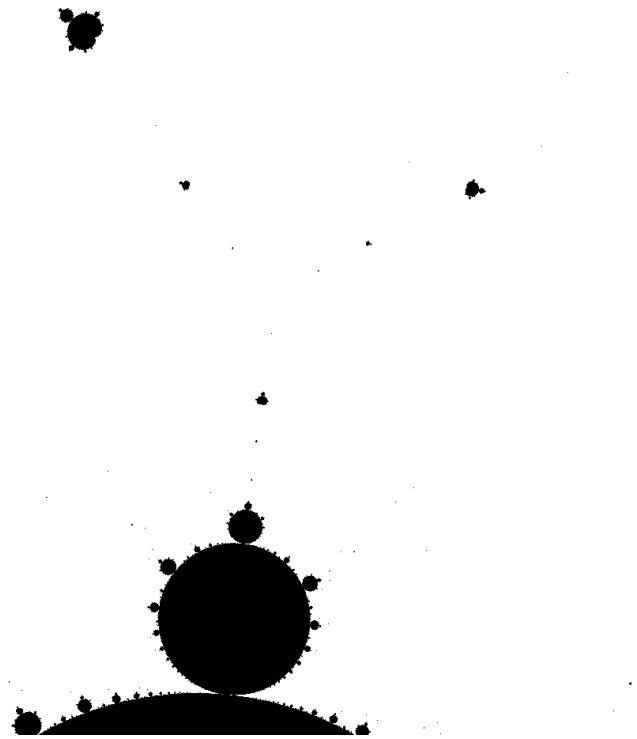

Fig. 12: "mandelbirds" in the classic Mandelbrot set, near the 3-cycle bulb at the bottom of this figure

Mandelbirds play an interesting role in the Mandelbrot set of $f_{bdm}(z)$ when intersected with the m-plane of (b,d,m) values. Associated with each bulb of the Mandelbrot set there is a pair of mandelbirds whose main cardioid is associated with the same period as the bulb. As the parameter φ varies from 0 to 2π, these two rotate about each other, making one half revolution in 2π radians. When the parameter r is varied, the pair of (rotating) mandelbirds is displaced nearer or further from the main cardioid of the Mandelbrot set. When r = 0.5, the mandelbird pair associated with the main cardioid of the Mandelbrot set rotates about a point on the edge of the main cardioid. This pair moves away or into that cardioid as r is increased or decreased from 0.5. For other bulbs of the Mandelbrot set, the associated mandelbird pair approaches the edge of the bulb for different values of r; for example the mandelbirds approach the edge of the 3-cycle bulb at

approximately r = 1.0. To see how the rotating mandelbirds approach the edge of a bulb, see the animation "Angry Mandelbirds".

When θ is varied, the pair of mandelbirds is displaced along a curve that can position them away from the associated bulb. In the case of the main cardioid, the pair is displaced along the edge of the cardioid, going around the cardioid from the points on the real axis -0.75 to 0.25 as θ goes from 0 to π, and continuing on the other side as θ continues to 2π. The mandelbirds associated with other bulbs follow different paths, depending on r. For example, the following images illustrate the paths followed by the mandelbirds associated with the 3-cycle bulb when r=1.0 and r=1.2:

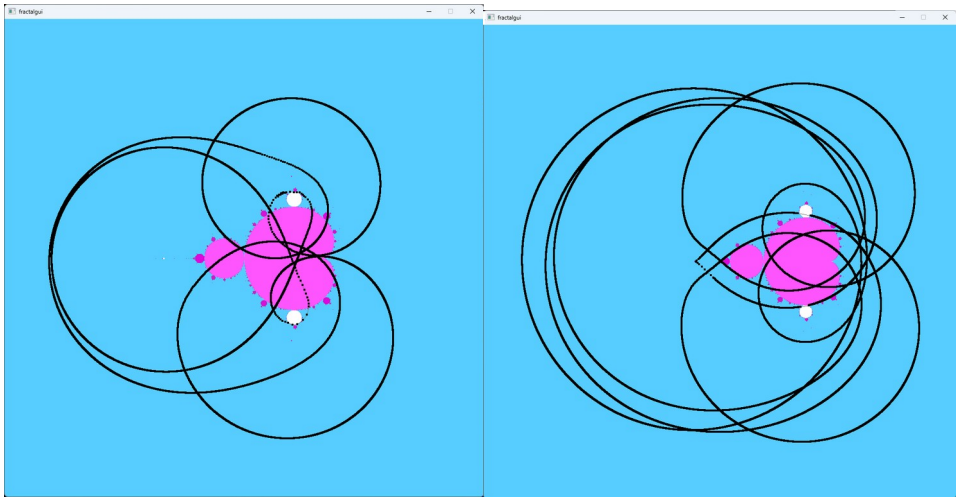

Figure 13: Paths followed by mandelbirds associated with 3-cycle bulbs, as θ is varied, with r = 1.0 and r = 1.2.

Note that θ may rotate several full rotations before a mandelbird pair is returned to its starting position, depending on the value of *r*.

Finally note that increasing or decreasing ε has the effect of shrinking or magnifying the size of the mandelbirds, as well as the distance between them, and also shrinks or magnifies the distortion of the Mandelbrot set bulb that occurs when the mandelbirds are near the associated bulb.

Why are we interested in these mandelbirds? The reason is that whenever a mandelbird is near its associated bulb, the edge of that bulb is distorted so as to reveal an MH curve. The Herman rings associated with that MH curve have the same period as is associated with the bulb. As a result we can find cyclic Herman rings of any period by finding where the mandelbirds associated with that period intersect the bulb of that period.

To illustrate the association between Herman rings and twirling pairs of mandelbirds, consider first the animation "Herman Rings on the Edge of the Mandelbrot Set" . This video shows the distortion to the main cardioid that occurs as θ varies from 0 to π, with r = 0.5. During the animation φ is initially equal to θ. When θ gets to π/6, θ is held constant while φ is rotated one revolution, to π/6 + 2π. During that rotation one can observe one of the two mandelbirds emerging from the main cardioid, circling clockwise before it disappears back into the cardioid. During that rotation, the MH ring is visible, but it sometimes passes through other bulbs of the Mandelbrot set. Both of the mandelbirds can be seen separate from the cardioid if r is slightly increased.

Another relevant example is shown in the animation "Angry Mandelbirds". This shows a pair of mandelbirds in the Mandelbrot set of $f_{bdm}(z)$ with r=1, ε=0.0002, with θ varying from π/12 to almost π/3 (56 degrees). During the animation, φ goes through about 80 revolutions, illustrating the distortion of the 3-cycle bulb as the rotating mandelbirds pass through that bulb. Note that as the mandelbirds approach the 3-cycle bulb, it distorts to reveal an MH curve near the edge of the bulb.

The "Angry Mandelbirds" animation only shows the MH curve that is not obscured by the 3-cycle bulb. The MH curve actually extends inside the bulb as well, although that portion of the MH curve is not visible in that animation. The Herman rings that occur along these MH curves are in a cycle of period 3. Herman rings from that bulb are illustrated in the video "Herman Rings in a 3-cycle". During that animation, sometimes the inside of the Herman rings contain a red-colored domain; at other times the inside contains a multitude of small blue domains. Whenever the MH curve is superimposed over the 3-cycle bulb, the resulting Herman ring cycle encircles a domain that is attracted to an attractive 3-cycle. When the MH curve is not superimposed over a bulb, the resulting Herman ring encloses a pattern of domains attracted to infinity. This is illustrated in figures 14 and 15:

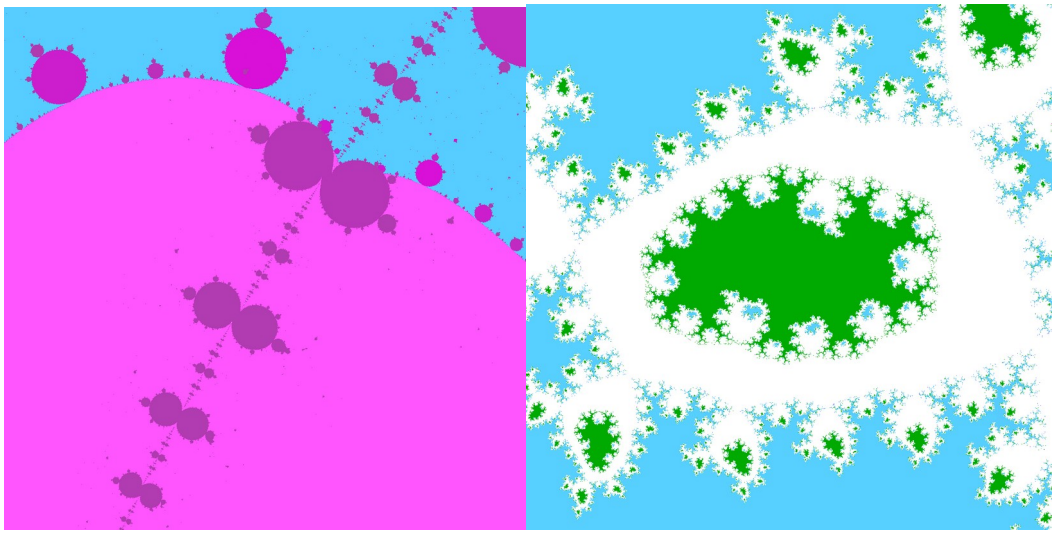

Figure 14: Mandelbrot set and Julia set for a Herman ring with interior a domain attracted to a fixed point. First image shows a Mandelbrot set of $f_{bdm}(z)$ showing an MH curve that lies on the central bulb (cardioid). Second image shows the Julia set associated with the point at the center of the first image, showing a Herman ring whose interior is filled with the domain of attraction to a fixed point.

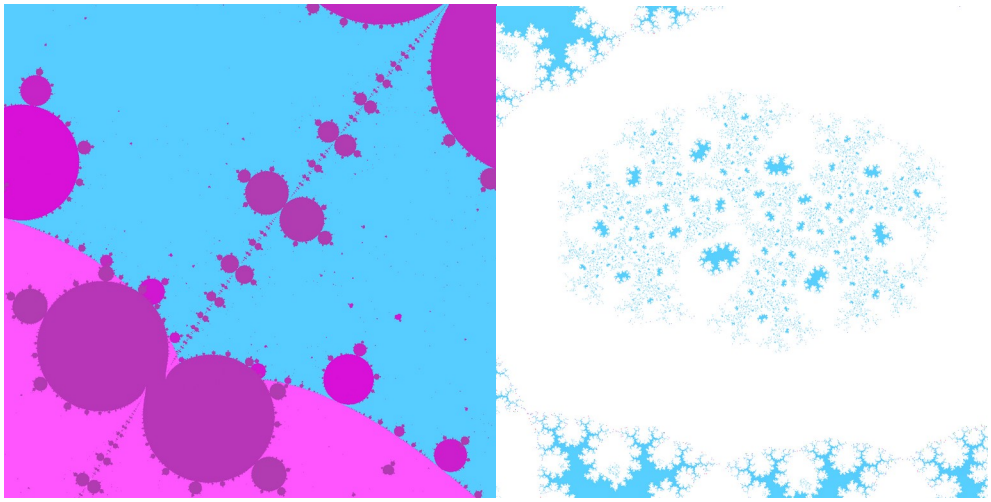

Figure 15: Mandelbrot set and Julia set for a Herman ring with interior not attracted to a fixed point. First image shows a Mandelbrot set of $f_{bdm}(z)$ showing an MH curve that does not lie on a bulb of the Mandelbrot set. Note that this image is near the first image of figure 14. Second image shows the Julia set associated with the point at the center of the first image,

showing a Herman ring whose interior is filled with many domains attracted to infinity

Whenever the interior of the Herman ring contains a repulsive fixed point, we can zoom into the fixed point, and every image containing the fixed point will contain a pattern of domains attracted to infinity. This can be useful in making animations that suggest endless travel through evolving fractal shapes. Consider for example the animation "A Flight through Spiral Clouds". During this animation, the Julia sets are defined by points along an MH curve of $f_{bdm}(z)$ that does not lie on a bulb or cardioid of the Mandelbrot set, so that the interior of the Herman rings contains a repulsive fixed point, but no attractive fixed point. The value of the fixed point is recalculated each frame and used as the center of the image of that frame. This zoom-in continues as far as double precision accuracy permits, to a 3-cycle on the MHRing, then it is followed by a zoom-out.

To summarize these observations:

1. When ε is small but nonzero, and for appropriate values of r (e.g. 0.5) , the m-plane of the Mandelbrot set of $f_{bdm}(z)$ is close to the classic Mandelbrot set, except for a small region near the edge of the classic Mandelbrot set.
2. By choosing appropriate values of r and θ, a pair of mandelbirds can be found near the edge of the Mandelbrot set, resulting in a warping of that edge, and an MH curve appears either inside or outside the edge of that Mandelbrot set.
3. The mandelbird pair associated with a bulb of the Mandelbrot set have the same period (in their central cardioids) as the period of the associated bulb of the Mandelbrot set.
4. As the angle φ passes through a rotation, the pair of mandelbirds travels approximately in a circular path. If these mandelbirds are near the edge of the associated bulb of the Mandelbrot set, that bulb will be distorted so as to reveal an MH curve. The points along that MH curve correspond to Herman rings having the same period as the period of the bulb.
5. The MH curve near the bulb of the Mandelbrot set can be either outside or inside the edge of the bulb, depending on the parameters b and d. When the MH curve is inside the edge of the Mandelbrot set, there is an attractive cycle (or fixed point) in the interior of the Herman ring. When it is outside, the interior of the Herman ring contains a cascade of similar shapes (preimages of the attractive basin of infinity). These shapes are repeated infinitely often in any neighborhood of the repulsive fixed points inside the Herman ring.

Other Mandelbrot sets for $f_2(z)$

The above techniques for finding Herman rings for $f_2(z)$ can be used to identify Herman rings whose formulas are near the complex plane of the classical Mandelbrot set of z^2+m, as $|b-d|$ approaches 0. It is easy to find additional Herman rings further from that complex plane by using the formula $f_2(z)=m+ z^2(z+b)/(\underline{b}z+1)$. We have already discussed this formula in the case that $m = 0$, where we found that $z^2(z+b)/(\underline{b}z+1)$ has Herman rings for many values of $|b|>3$. The MH curve of this formula can also be seen in the complex plane of m-values. The animation "Rings Rolling along a Mandelbrot Set" illustrates the intersection of the m-plane with the Mandelbrot sets of $m+ z^2(z+b)/(\underline{b}z+1)$ as b rotates about the circle of radius 3.1 about the origin. In that animation the image center is always the value $m=0$, however the MH curve in the m-plane extends to other values of m, showing that this MH hypersurface includes Herman rings that were not derived from the formula $z^2(z+b)/(\underline{b}z+1)$.

The Herman rings associated with $m+ z^2(z+b)/(\underline{b}z+1)$ are a small subset of those associated with $m+ z^2(z+a)/(bz+1)$. When $|a|$ and $|b|$ are at least 3, there is visible an MH curve in the m-plane, whenever $arg(a)$ is near $-arg(b)$, i.e. when b is not too far from $\underline{a}$. The Herman rings associated with this function $f_2(z)$ appear similar to those observed before with $f_1(z)$.

In addition one can identify the functions $f_1(z) = z^2(z+b)/(1+cz)$ as the subset of the functions $f_2(z)$ having m = 0. This set of Herman rings is not limited to just functions with m=0; the MH curves that occur when m = 0 also extend to nonzero values of m.

7. Mandelbrot sets and Herman rings of $f_3(z)=mz(1-z)(az+b)/(cz+d)$

This function provides a different parameterization of degree 3 rational functions having denominator of degree one. Similar to the discussion about $f_2(z)$ above, this family of rational functions can be reduced to $f_3(z) = mz(1-z)(z+b)/(z+d)$, with complex numbers b, d and m. The formula $f_3(z)$ reduces to the standard quadratic $mz(1-z)$ (known as the lambda mapping, with $\lambda=m$) when b approaches d. This mapping exhibits similar behaviors to $f_2(z)$ with a few additional useful properties. As above we replace b and d with polar coordinates, using r, ε, θ, and φ, with $b-d$ equal to $2\varepsilon e^{i\varphi}$ where $|b-d| = 2\varepsilon$, and representing $b+d$ as $2re^{i\theta}$ where $|b+d| = 2r$, with θ and φ real values between 0 and 2π, and r and ε real numbers.

Much of the discussion of section 6 is also relevant for $f_3(z)$, in the sense that twirling mandelbirds can be used to find periodic cycles of Herman rings for $f_3(z)$. When ε is small this Mandelbrot set is similar to the quadratic Mandelbrot set (in λ coordinates). For each bulb of the Mandelbrot set of $mz(1-z)$ there is a pair of mandelbirds in the Mandelbrot set of $f_3(z)$. The parameters r and θ can be chosen so that the mandelbirds approach the edge of the bulb. while the mandelbirds spin in a circular pattern as φ goes from 0 to π. When the mandelbirds are near the edge of the associated bulb, that bulb distorts in such a way so as to reveal an MH curve, associated with Herman rings having the same period as the bulb.

The same techniques used for finding periodic cycles of Herman rings for $f_2(z)$ are also used with $f_3(z)$ to animate a 6-cycle of Herman rings, shown in the video "Six-cycles of Herman Rings". Similarly a three-cycle of Herman rings is shown to bifurcate into a 9-cycle of Herman rings in the video "A Three to Nine cycle Herman Ring Transition".

There is however one significant useful difference between the Mandelbrot sets of $f_2(z)$ and $f_3(z)$. Recall that when r=0.5, the main cardioid of $f_2(z)$ becomes distorted in a small region whose location depends on the value of θ, rotating around the cardioid as θ goes from 0 to 2π, displaying an MH curve for a short interval depending on θ. In contrast, with the Mandelbrot set of $f_3(z)$, a single MH curve follows along the edge of the unit circle, wrapping almost all the way around, when r is approximately 0.1 and $0< \varepsilon < r/2$. When $|\varphi-\theta|=\pi$, the MH curve is inside the main bulb of the Mandelbrot set, and when φ =θ, the MH curve is outside the bulb. When |φ-θ| is about π/2, the MH curve overlaps the edge of the main bulb. These cases are illustrated below:

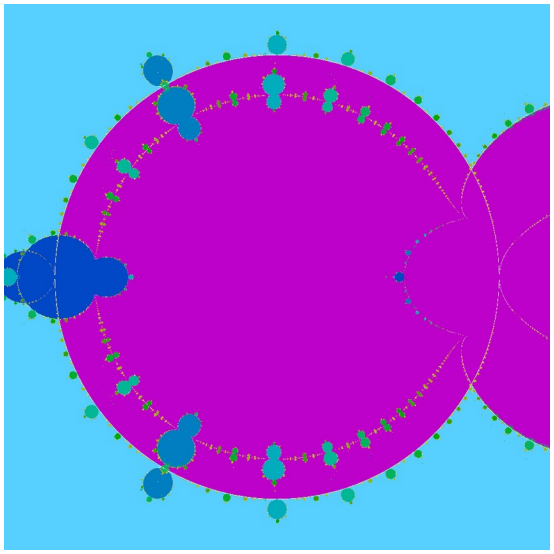

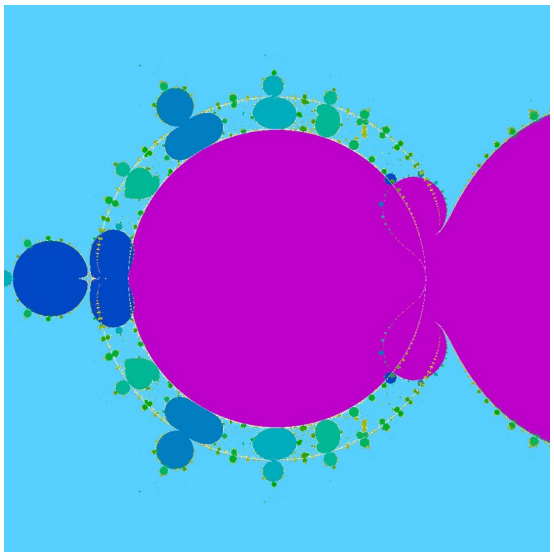

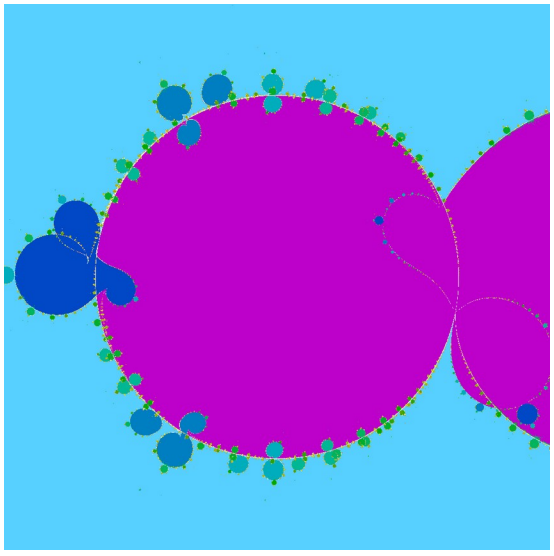

Figure 16: Mandelbrot sets for $f_3(z)$, with r=0.1 and ε=0.01, and φ=0. In the first image, θ=π, so that the MH curve is inside the main bulb. In the second image, θ=0, resulting in the MH curve outside the main bulb. The third image shows the MH curve approximately coinciding with the edge of the bulb, when θ=π/2.

The video "Exploration of a Mandelbrot set with Herman rings along a circle" illustrates this Mandelbrot set, showing MH curves that can be found by varying φ and θ.

The MH curve can be made to coincide with the edge of the main bulb by slight adjustment of φ near φ= θ+ π/2. When these two curves coincide, the same Julia set will have both a Herman ring and Siegel disc, with the Siegel disc in the interior of the Herman ring. The video "Siegel discs in Herman rings" shows the Julia sets with both Herman rings and Siegel discs as their winding numbers are varied. To visualize a Julia set where the Herman ring contains a Siegel disc, one can calculate a Mandelbrot set image where the MH curve nearly overlaps with the edge of a bulb as in the following image:

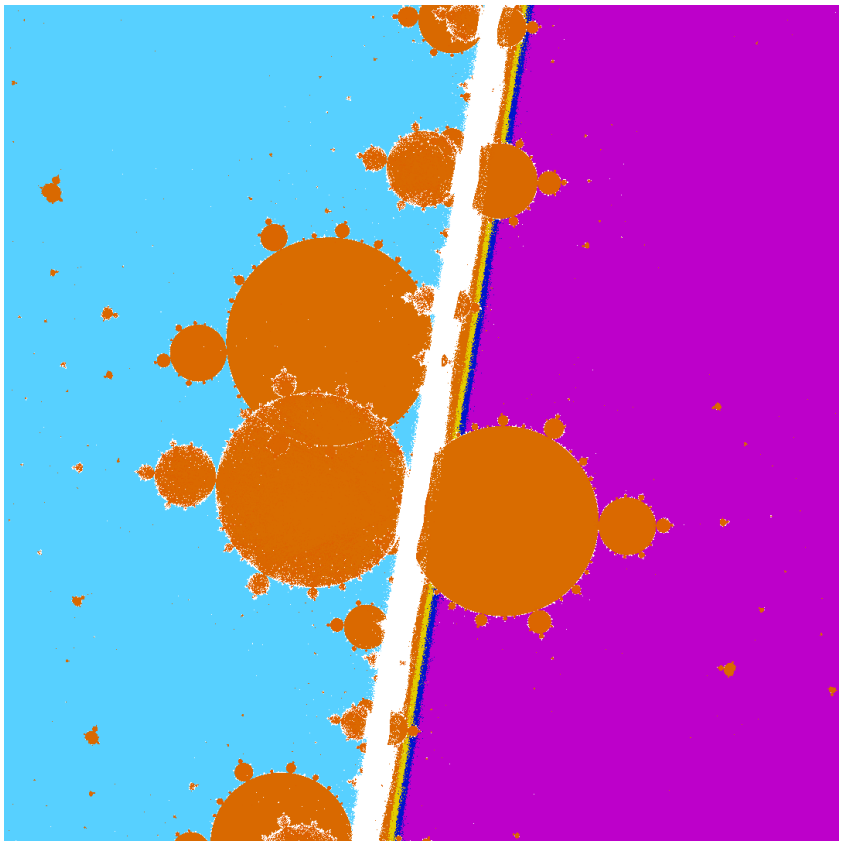

Figure 17: Mandelbrot set for $f_3(z)$, where an MH curve nearly coincides with the edge of the bulb associated with an attractive

cycle. To cause the Siegel disc to appear inside the Herman ring, the parameter φ is calculated to make the two curves coincide.

One can determine the value of φ needed to make the two curves coincide by determining the radii of the two curves associated for two nearby values of φ and then (assuming the radius varies linearly with φ, which is approximately true) solve for the desired value of φ. Repeating this operation two or three times results in a value for which the associated Julia set will show the Siegel disc inside the Herman ring. Constructing the video "Siegel discs in Herman rings" required solving for φ at 30-40 different points around the MH curve, and interpolating φ along the MH curve.

A different parameterization for Herman rings from $f_3(z)$.

The techniques described above for constructing Herman rings using the function $f_3(z)$ are only useful when $|b-d|$ is small, so we are only finding Herman rings in a small subset of these functions. Another (easy) way to find Herman rings in the space of functions $f_3(z)$ is to consider the functions

$f_3(z) = mz(1-z)(z+b)/(1+cz).$

This can be compared with the discussion of $f_2(z)=m+ z^2(z+b)/(cz+1)$ above. With both $f_2(z)$ and $f_3(z)$, when |b| and |c| are sufficiently large (say greater than 5) there exist MH curves in the m-plane that are approximately circular, which are degenerate for some values of arg(b) and arg(c) but are quite apparent when b and c are real.

When b and c are sufficiently large the Mandelbrot set for $f_3(z)$ shows an approximately circular MH curve, which is easily found in either the m-plane or the b-plane, as shown below:

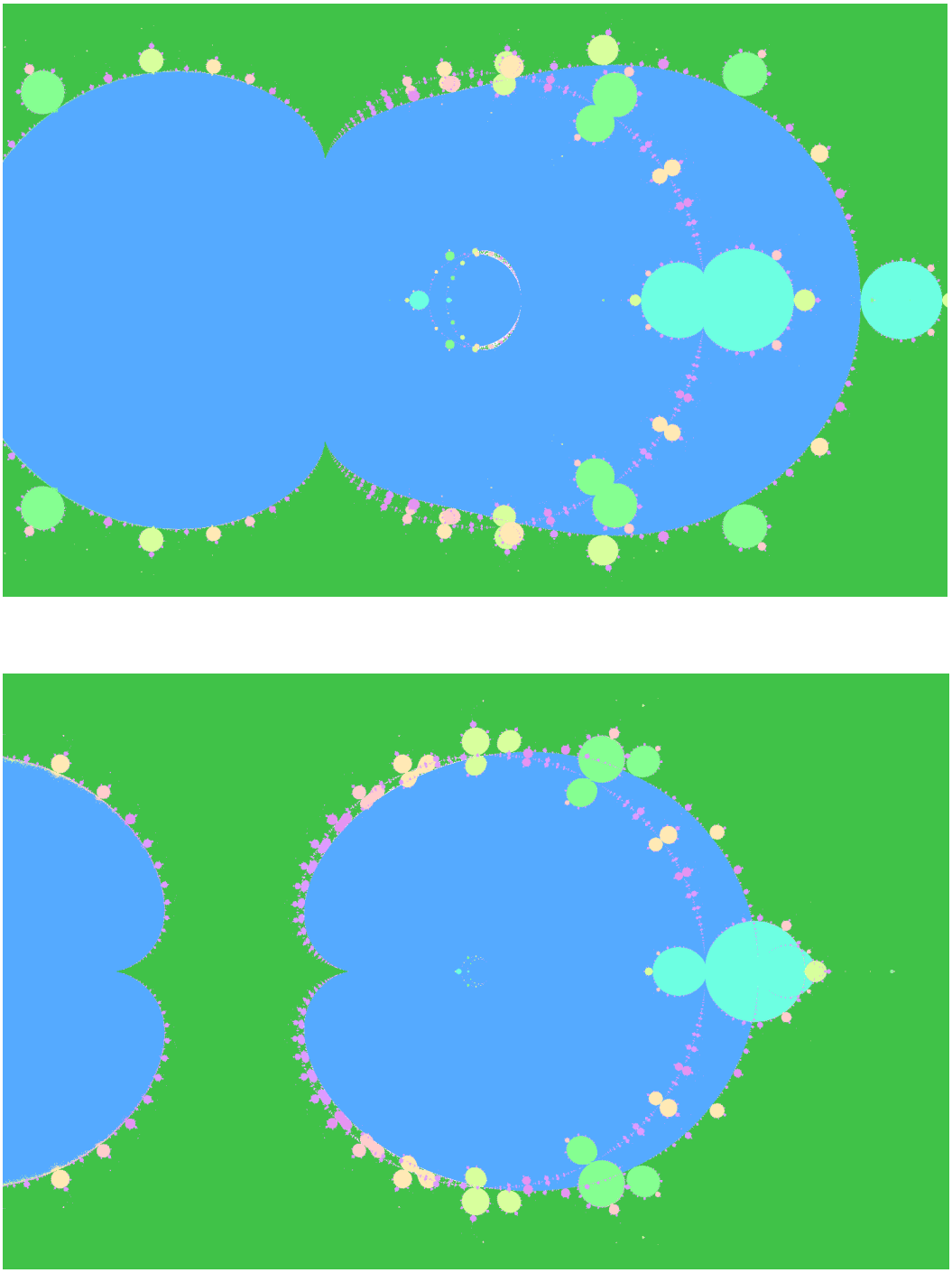

Figure 18: Mandelbrot sets for the functions $f_3(z) = mz(1-z)(z+b)/(1+cz)$. The first image shows the m-plane, with b=8 and c=5. The second image shows the b-plane with c=16 and m=1.

8. Rational functions with denominator of degree 2

When we relax the requirement that infinity be superattractive, there is a four (complex)-dimensional space of third degree rational functions that can be expressed as either

$g_1(z)=x(x+a)(x+b)/(cx+1)(x+d)$ or

$g_2(z)=x(x+a)(x+b)/(cx+1)(dx+1)$

These two forms, although equivalent, are helpful in identifying two different families of Herman rings.

Compared to using the functions f(z) with infinity superattractive, the most important difference is that for the functions g(z), infinity may or may not be attractive. Let N be the leading coefficient of the numerator and D be the leading coefficient of the denominator. Then infinity is attractive whenever $|N/D|>1$, and it is repulsive whenever $|N/D|<1$. Similarly, let n be the constant coefficient of the numerator and let d be the constant coefficient of the denominator. Then zero is attractive when $|n/d|<1$, and zero is repulsive when $|n/d|>1$.

While the attraction to infinity and zero is not very important from the point of view of the complex dynamics (zero and infinity are just two different points on the Riemann sphere), these are important in determining the appearance of the Julia sets that are visualized in the complex plane. For example, when infinity is repulsive, it will lie in the Julia set, and if there are Herman rings, they will be endlessly repeated as you visualize larger and larger domains. When infinity is attractive, the Julia sets are similar to the superattractive case, and the interesting components of Julia sets will all appear in a finite domain.

MH curves associated with $g_1(z)=z(z+a)(z+b)/(cz+1)(z+d)$

Recall the technique used above to find periodic cycles for $f_2(z)$ and $f_3(z)$: In both cases the formula $(z+b)/(z+d)$ was multiplied by a quadratic polynomial used to calculate a quadratic Mandelbrot set. When $|b-d|$ approaches 0, the formula reduces to the quadratic polynomial for which the Mandelbrot set is known. We found that, when $|b-d|$ is small, MH curves can be found near the bulbs of the quadratic Mandelbrot set, with periodic Herman rings having the same period as the corresponding bulbs of the quadratic Mandelbrot set. This enables us to identify periodic cycles of Herman rings in the Mandelbrot sets of $f_2(z)$ and $f_3(z)$.

A similar technique can be used to find Herman rings of the formula $g_1(z)$. We can start with the second degree rational function $r(z)=z(z+a)/(cz+1)$. That formula has a Mandelbrot set in complex 2-

space that can be visualized by varying c over time, animating the planar images associated with this formula in the plane of *c*. This can be seen in the video "Rocking and Rolling with Mandelbrot". If one chooses the value c = -2, there is a period-2 bulb whose edge is seen in the following image:

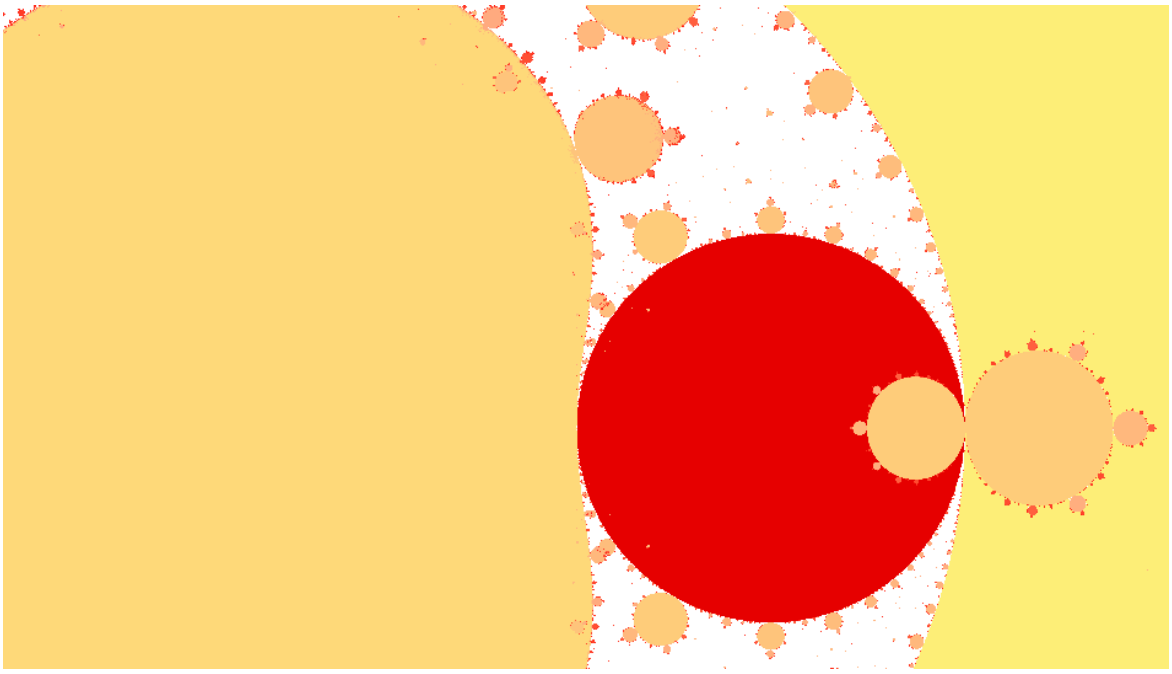

Figure 19: The Mandelbrot set of $z(z+a)/(cz+1)$, along the slice $c = -2$.

The above slice through the Mandelbrot set of $r(z)$ with c = -2, centered at the value a=(-.953, -.469), shows the edge of the 2-cycle bulb on the left side of this figure.

For comparison, the following is the Mandelbrot set of $g_1(z)$, with the same value of c, centered at the same value of a, but with values of b and d chosen with $|b-d|=.001$:

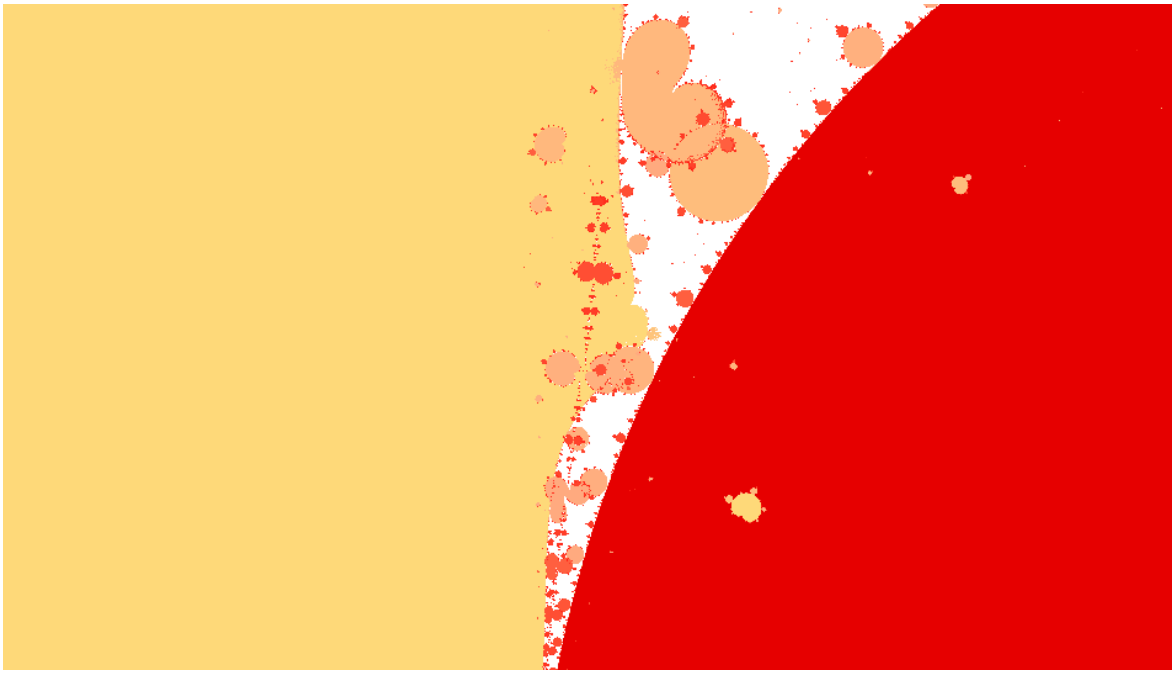

Figure 20: An MH curve for $g_1(z)$, near the edge of the 2-cycle bulb of $r(z)$.

The second image has also been magnified by a factor of about 4 so that one can see an MH curve along the edge of the 2-cycle bulb. A mandelbird is also visible, an angle of 155 degrees was used to obtain the bulge in the 2-cycle bulb needed to expose the MH set, in the same way as we positioned mandelbirds near the 3-cycle bulb to expose an MH set for the function $f_2(z)$ previously. By choosing values of a,b,d along the MH curve in figure 20, one obtains a Julia set of $g_1(z)$ having a cyclic period-2 Herman ring, as illustrated below:

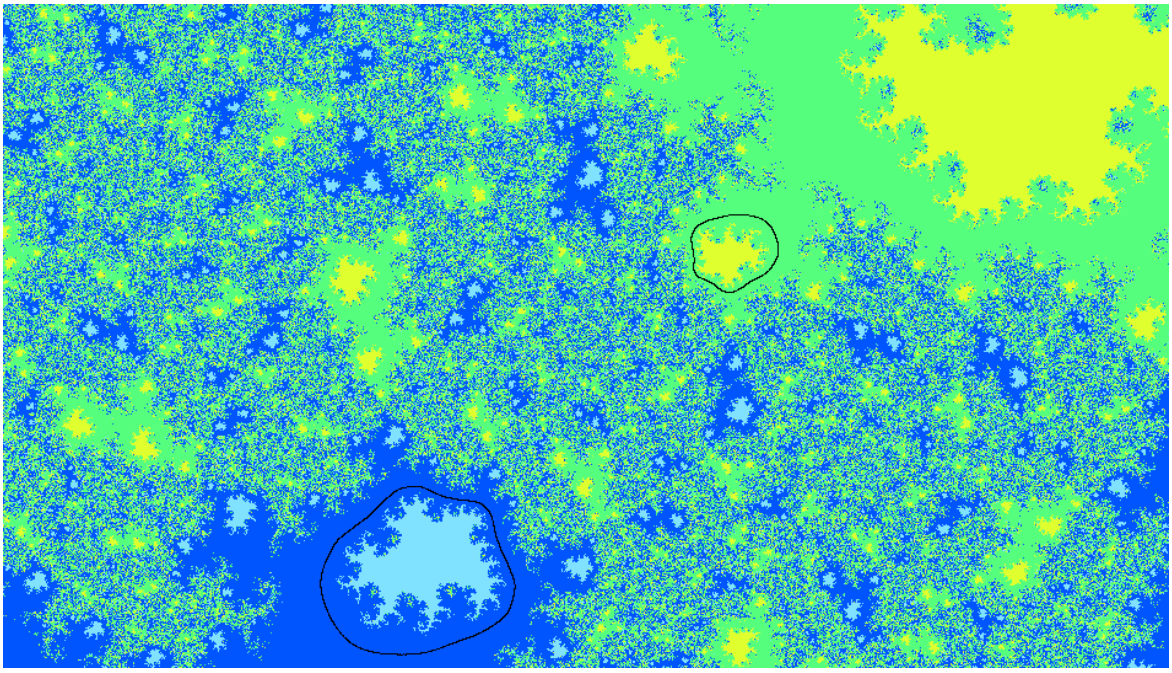

Figure 21: A period-2 Herman ring for $g_1(z)$, identified using the MH curve in figure 20.

In the above image, the period-2 Herman ring cycle is illustrated with two black rings. The preimages of the periodic Herman ring are colored darker shades of green and blue. The yellow and light blue colors indicate points in the interior of the Herman ring that converge to the 2-cycle of points in the Herman ring. Note that in this case $|c|>1$ and $|a|>1$ so that both zero and infinity are repulsive. As a result the complex plane is filled with preimages of the Herman ring cycle and its interior. The animation "Endless Rings Filling the Plane" results from following this MH curve along the edge of the 2-cycle region. That animation performs a zoom toward the origin, while the value of a follows along the MH curve.

MH curves associated with $g_2(z)=z(z+a)(z+b)/(cz+1)(dz+1)$

The MH curves of $g_1(z)$ described above are all located very close to the edges of bulbs of the Mandelbrot set of $r(z)=z(z+a)/(cz+1)$. There is also another MH hypersurface that is not close to the Mandelbrot set of r(z), which provides Herman rings appearing different from the other Herman rings we have seen. These MH curves are easily identified using the function

$$g_2(z)=z(z+a)(z+c)/(bz+1)(dz+1)$$

An approximately circular MH curve occurs in the plane of a-values when c is chosen to be a real value larger than 3, and b and d are

chosen to be real values less than 0.5. For example the following MH curve (of radius approximately 10) occurs with c=10, b=d=0.1:

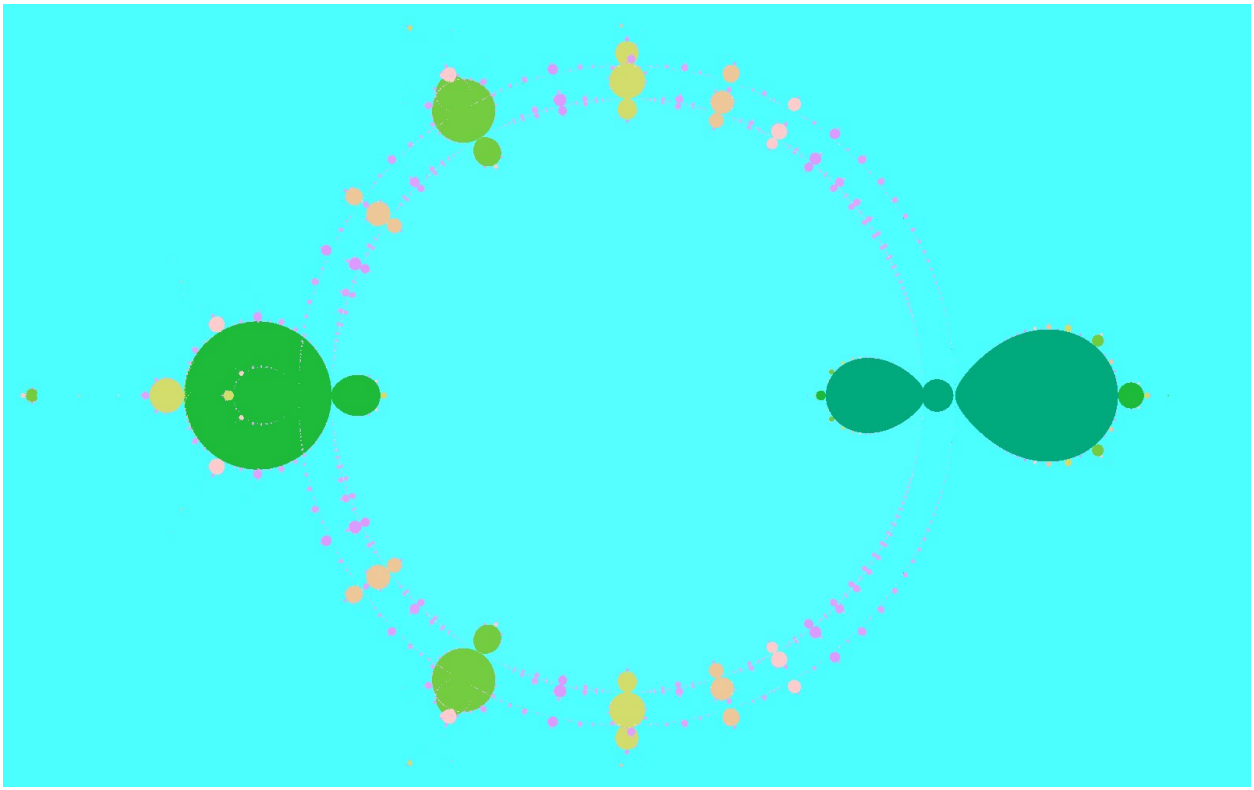

Figure 21: A near-circular MH set in the a-plane associated with $g_2(z)$, with c=9, b=d=0.1.

When the arguments of *b,d,c* are varied (making these parameters non-real), a similar MH curve occurs in the a-plane, but with some distortion and rotation.

The Julia sets associated with points along these MH curves are sometimes similar to the Julia sets we have seen from *f(z)*, however they can be very different, especially with larger values of *d*. See for example the video "Squirmy Critter" which follows the MH curve with */a/*and */c/* approximately 3, *b=d=0.3*, with values of *a* chosen from the MH curve. The resulting Julia sets stretch out linearly for some values of *c*, and become symmetric around the Herman ring at other values.

9. Summary of MH sets identified in 3rd degree rational functions

$f_1(z)= z^2(z+b)/(cz+1)$: When */b/* and */c/* are greater than 3 there is an approximately circular MH curve for this function. That MH curve is shown in the video "A Breakup in a Mandelbrot Set for Herman Rings".

$f_2(z) = m + z^2(az+b)/(cz+d)$:

When m is near 0, the MH curves associated with $f_1(z)$ extend into the space of $f_2(z)$.

When $a=c=1$ and $|b-d|$ is small, MH curves can be found near the bulbs of the classical Mandelbrot set, indicating the presence of periodic cycles of Herman rings. This is illustrated in the video "Herman Rings on the Edge of the Mandelbrot Set, as well as in the video "Angry Mandelbirds".

When $a=d=1$ and b is near c, a ring of MH curves follows the edge of the Mandelbrot set. This is illustrated in the video "Rings Rolling along a Mandelbrot Set" .

$f_3(z) = mz(1-z)(az+b)/(cz+d)$:

When $a=c=1$ and $|b-d|$ is small, MH curves can be found near the bulbs of the classical Mandelbrot set (lambda coordinates), indicating the presence of periodic cycles of Herman rings. This is illustrated in figure 16.

When $a=d=1$ and $|b|$ and $|c|$ are larger than 4, a ring of MH curves is near the edge of the Mandelbrot set (lambda coordinates), and can be made to intersect that edge for appropriate values. This is illustrated in figure 18.

$g_1(z)=z(z+a)(z+b)/(zx+1)(z+d)$:

When$|b-d|$ is small, MH curves can be found near the bulbs of the Mandelbrot set for $z(z+a)/(cz+1)$. This is illustrated in figure 20. These curves identify periodic cycles of Herman rings corresponding to the same period as the nearby bulb of the Mandelbrot set for $z(z+a)/(cz+1)$.

$g_2(z)=z(z+a)(z+b)/(cz+1)(dz+1)$:

For fixed a,b and c, an approximately circular MH set can be found in the d-plane, as shown in figure 21.

Conclusions

Herman rings were found to occur along MH hypersurfaces in various generalized Mandelbrot sets of third degree rational functions. To find the parameters that determine a function that has a Herman ring, we use a generalization of the Mandelbrot set. That generalization can be used to

construct curves (MH curves) in the parameter spaces of these functions, that follow along as the Herman rings evolve. These curves can be used to animate Julia sets and their Herman rings.

Five families of third degree rational functions were discussed above:

$f_1(z) = z^2(az+b)/(cz+d)$,

$f_2(z) = m+ z^2(az+b)/(cz+d)$

$f_3(z) = mz(1-z)(az+b)/(cz+d)$,

$g_1(z)=z(z+a)(z+b)/(cz+1)(z+d)$

$g_2(z)=z(z+a)(z+b)/(cz+1)(dz+1)$

These five all have Julia sets with Herman rings, found by identifying MH curves in the complex spaces of the parameters defining the functions.

Several features of the generalized Mandelbrot sets and their Herman rings were identified, including:

MH surfaces and curves were found useful for locating Herman, and these Herman rings can be animated by choosing points along the MH curves.

Separation of bulbs along MH curves were shown to be associated with the alignment of spirals on opposite sides of the Herman ring.

Twirling mandelbird pairs were found useful in identifying MH curves on the edges of bulbs of generalized Mandelbrot sets.

Periodic cycles of Herman rings of arbitrary period were found associated with $f_2(z)$, $f_3(z)$, and $g_1(z)$, by use of twirling mandelbird pairs.

Patterns were found in which Herman rings and their preimages converge to repulsive fixed points of rational functions, and in which the Herman ring preimages fill the complex plane.

A diversity of interesting and attractive fractal shapes is revealed by the use of MH curves and generalized Mandelbrot sets in spaces of degree 3 rational functions.